Design Synthesis of Articulated Heavy Vehicles with Active Trailer Steering Systems

by

Md. Manjurul Islam

A thesis

presented to the University of Ontario Institute of Technology

in fulfillment of the

thesis requirement for the degree of

Master of Applied Science

in

Automotive Engineering

Oshawa, Ontario, Canada, 2010

AUTHOR'S DECLARATION

I hereby declare that I am the sole author of this thesis. This is a true copy of the thesis, including any required final revisions, as accepted by my examiners.

I understand that my thesis may be made electronically available to the public.

Abstract

A new design synthesis method for articulated heavy vehicles (AHVs) with an active trailer steering (ATS) system is examined and evaluated. Due to their heavy weights, large sizes, and complex configurations, AHVs have poor maneuverability at low speeds, and low lateral stability at high speeds. Various passive trailer steering and ATS systems have been developed for improving the low-speed maneuverability. However, they often have detrimental effects on the high-speed stability. To date, no systematic design synthesis method has been developed to coordinate the opposing design goals of AHVs. In this thesis, a new automated design synthesis approach, called a Single Design Loop (SDL) method, is proposed and investigated. The SDL method has the following distinguished features: 1) the optimal active design variables of ATS systems and the optimal passive vehicle design variables are searched in a single design loop; 2) in the design process, to evaluate the vehicle performance measures, a driver model is developed and it 'drives' the vehicle model based on the well-defined testing specifications; and 3) the ATS controller derived from this method has two operational modes: one for improving the lateral stability at high speeds and the other for enhancing path-following at low speeds. To demonstrate the effectiveness of the new SDL method, it is applied to the design of an ATS system for an AHV with a tractor/full-trailer. In comparison to a conventional design approach, the SDL method can search through solutions in a much larger design space, and consequently it provides a more comprehensive set of optimal designs.

Acknowledgements

I would like to thank my supervisor Dr. Yuping He for his encouragement, support and guidance during my thesis work. I would also like to thank my supervisory committee members Dr. Ghaus Rizvi and Dr. Hossam Kishawy for serving on my thesis committee and making significant contribution to enhance the quality of this work. Financial support of this research by the Natural Science and Engineering Research Council of Canada and Genist Systems Company is gratefully acknowledged.

Dedication

I would like to thank also my mom and dad for their unconditional love, affection and support in my life.

Table of Contents

List of Figures

List of Tables

Nomenclature

C_1	Cornering stiffness of the front tire of tractor
C_2	Cornering stiffness of the rear tire of tractor
C_3	Cornering stiffness of the front tire of trailer
C_4	Cornering stiffness of the rear tire of trailer
$d=S_1+S_2$	
$e=S_3+S_4$	
F_x	Longitudinal hitch reaction force of tractor
F_y	Lateral hitch reaction force of tractor
$F_{y1}(\alpha_1)$	Lateral force acted on the front axle of tractor
$F_{y2}(\alpha_2)$	Lateral force acted on the rear axle of tractor
$F_{y3}(\alpha_3)$	Lateral force acted on the front axle of trailer
$F_{y4}(\alpha_4)$	Lateral force acted on the rear axle of trailer
I_1	Principal yaw mass moment of inertia of tractor
I_2	Principal yaw mass moment of inertia of trailer
m_1	Total mass of tractor
m_2	Total mass of trailer
S_1	Distance between front axle and centre of gravity (CG) of tractor
S_2	Distance between rear axle and CG of tractor
S_3	Distance between hitch and rear tire of tractor
S_4	Distance between front tire of trailer and hitch
S_5	Distance between front axle and CG of trailer
S_6	Distance between rear axle and CG of trailer
U_1	Longitudinal speed of tractor
U_2	Longitudinal speed of trailer
V_1	Lateral speed of tractor
V_2	Lateral speed of trailer
x_1-y_1	Body fixed coordinates for tractor
x_2-y_2	Body fixed coordinate system for trailer
α_1	Side-slip angle of front tire of tractor
α_2	Side-slip angle of rear tire of tractor

α_3	Side-slip angle of front tire of trailer
α_4	Side-slip angle of rear tire of trailer
δ	Steering angle of front tire of tractor
δ_r	Steering angle of front tire of trailer
ω_1	Yaw rate of tractor
ω_2	Yaw rate of trailer
ψ	Articulation angle between tractor and trailer

Chapter 1

INTRODUCTION

1.1 WHY ARE ARTICULATED HEAVY VEHICLES WIDELY USED?

The majority of articulated heavy vehicles (AHVs) are commonly used for the transportation of goods and materials because of their cost effectiveness in both labor requirements (mainly the driver) and fuel consumption. An AHV is a substitute to a number of single units, since it is an assemblage of two or more rigid (*i.e.* non-articulating) vehicle units [1]. An AHV, therefore, moves more payloads with lower tare weight than a single unit vehicle, with only one driver. Moreover, compared with single unit vehicles, AHVs greatly reduce greenhouse gas emissions. Thus, the trucking industry all around the world has demonstrated incredible commercial attractiveness of AHVs.

1.2 VEHICLE CONFIGURATIONS

In an AHV, adjacent units are connected through mechanical couplings, such as pintle hitches, dollies, and 5^{th} wheels. The towing unit is called tractor and it usually has one or more steerable axles controlled by the driver. Each of the following vehicle units is called a trailer. There are two major groups of trailers: semi-trailers andfull trailers. A semi-trailer is supported vertically by its tractor at the front and the rear end is connected to the rear running gear. In afull trailer, on the other hand, the front support from the towing unit is replaced by its front running gear.

1.3 MOTIVATION

The popularity and application of AHVs is growing rapidly because of their great commercial benefits. However, the handling characteristics of AHVs are more complex than those of single unit vehicles, as neighboring units affect each other due to inner forces acting at their articulated point [2]. In addition to this, due to their large sizes and heavy weights, the operation of AHVs has been of primary concern to highway safety [3]. Consequently, the design of an AHV is a challenging task. The key reason of AHVs' intricate dynamics is the articulated joints through which the neighboring vehicle units interact with each other. The distinguished dynamics features of AHVs may lead to unstable motion modes [4]. These unstable motion modes may cause hazardous accidents. In the US, more than 35,000 people were killed in road accidents each year from 1993 to 1998 [5]. Among them, about 10% were the results of the unstable motion modes of AHVs. These unstable motion modes become dominant at high speeds.

The unstable motion modes of AHVs can be classified into three types. The first type is called *jack-knifing*, mainly caused by the uncontrolled large relative angular motion between adjacent units. It often results in the lateral slip of rear axles of the leading unit. The jack-knifing motion mode is a main reason for dangerous traffic accidents. When the articulation angle reaches a certain limit, it becomes incredibly difficult for the driver to control the vehicle by steering the tractor.

The second type of unstable motion modes is the *lateral oscillation* of trailers, called trailer sway. This unstable motion mode is usually experienced when design variables

and/or operating parameters are chosen very close to their critical values. In this case, a very little amount of disturbances acting on the vehicle, *e.g.*, side wind gust, abrupt steering effort by the driver, etc., may cause the lateral oscillation [6]. This may result in the loss of stability and the vehicle becomes self-excited due to non-conservative forces [7]. For AHVs, these non-conservative forces may arise at the contact point between tire and road due to lateral forces, aligning torques and longitudinal forces [8].

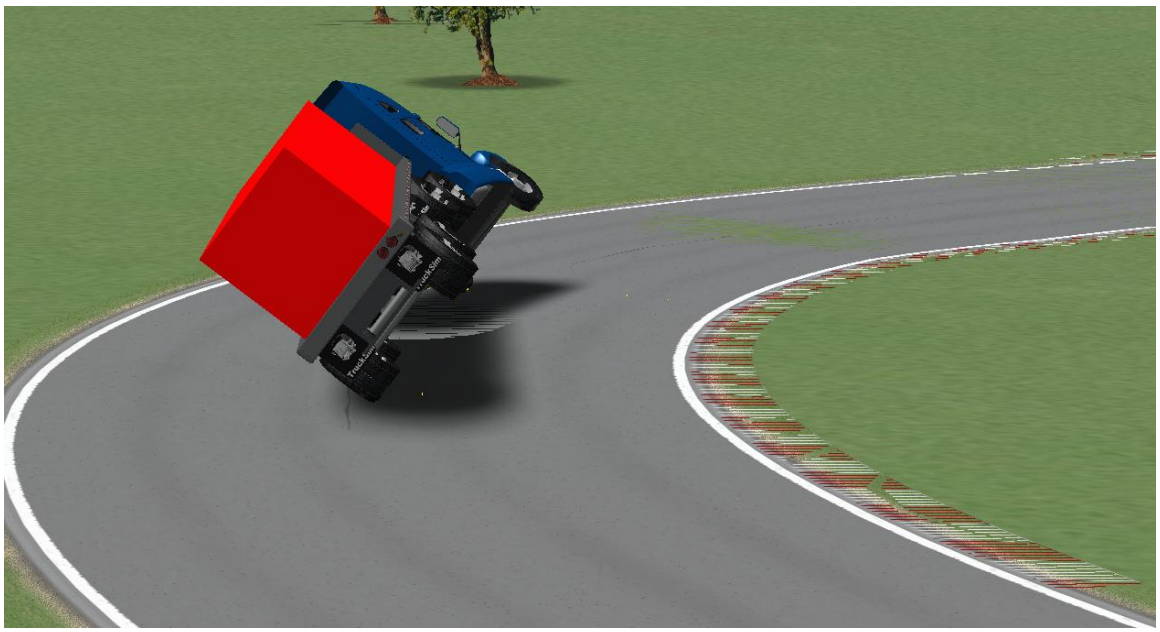

Fig. 1.1: Roll-over of an AHV during high-speed turning maneuver

The third type of AHV unstable motion modes is called *roll-over*. An example of this unstable motion mode is shown in Fig. 1.1. It is a worldwide safety problem with a fatality rate higher than any other type of accidents [16]. In Canada, 45% of accidents associated with the transportation of dangerous liquids occurred due to AHV roll-over, and 72% of the accidents took place while negotiating a curve [18]. Another study reports

that in the UK, 573 AHV accidents involved rollover in 2001 [17]. Recently, the US Department of Transportation has reported that in the USA roll-over accidents account for around 50% of the 700 annual heavy duty truck fatalities [18].

It is difficult for the driver to sense the roll-over unstable motion mode. The driver perception is mainly based on the response of the tractor, rather than trailers [15]. In an AHV, the rearmost trailer is usually the unit to roll-over first. By the time the driver realizes the rollover occurrence, it usually becomes too late for the driver to take corrective control action. During a lane change maneuver, roll-over accidents of AHVs occur when centrifugal forces destabilize the vehicle. At this time, three forces act on the vehicle, i.e. tire forces, centrifugal forces, and gravitational forces. The tire forces act on the horizontal level and push the vehicle towards the center of the path. The centrifugal forces are parallel to the ground and pass through the centers of gravity (CG) of the vehicle units in the direction opposite to the one it is turning. These two forces make a resultant torque to enhance the vehicle roll towards the outside of the curve. The gravitational forces act downward through the CG of the vehicle units. When the tire and centrifugal forces are large enough to overcome the force of gravity, the vehicle starts to roll-over.

AHVs' lateral stability at high speeds, in particular, roll-over, is highly dependent on an important dynamic performance measure called Rear-Ward Amplification (RWA) ratio [26]. The significance of RWA implies the tendency for the rearmost trailer to have a higher lateral acceleration than that of the vehicle's towing unit [1]. RWA ratio is

defined as the ratio of the peak lateral acceleration at the rearmost trailer's CG to that of the vehicle's towing unit in an obstacle avoidance lane-change maneuver [4, 27]. In a general sense, the lower the RWA ratio, the higher the vehicle lateral stability [55].

The above unstable motion modes refer to high speed directional performance issues. Interestingly, the high speed issues of AHVs are conflicting with those at low speeds in meeting the relevant AHV standards. Australian performance-based standards (PBS) [36], for example, describes the performance issues related to both high- and low-speed AHV operations. At low speeds the main directional performance measure is the path-following ability of rearmost unit. In general, AHVs' rear unit faces difficulties in tracking the lead unit's path. In an AHV, where the rearmost axle cannot steer during a turn, the rear tires follow different paths as from those of the steering tires of the towing unit. The commonly used performance measure for low-speed path-following is called *Path-Following Off-Tracking (PFOT)* [1]. This PFOT has been observed since the first time multi-axle vehicles were built [22].

AHVs' complex configurations and large sizes lead to poor path-following performance while traveling at low speeds on a local road and city streets [10]. The amount of PFOT of each unit is proportional to the square of its wheelbase [1]. This poor path-following ability is the source of tire scrub against the road during tight cornering maneuvers. The tire scrub damages both the tire and road surfaces [28]. Moreover, inferior path-following capability of AHVs rises safety concerns for the neighboring traffic and damage of road infrastructure [29]. PFOT is defined as the maximum radial

offset between the path of the tractor's front axle centre and that of the trailer's rear axle centre during a specific maneuver [30]. Note that besides wheelbase the PFOT is also dependent on other factors, such as forward speed [21].

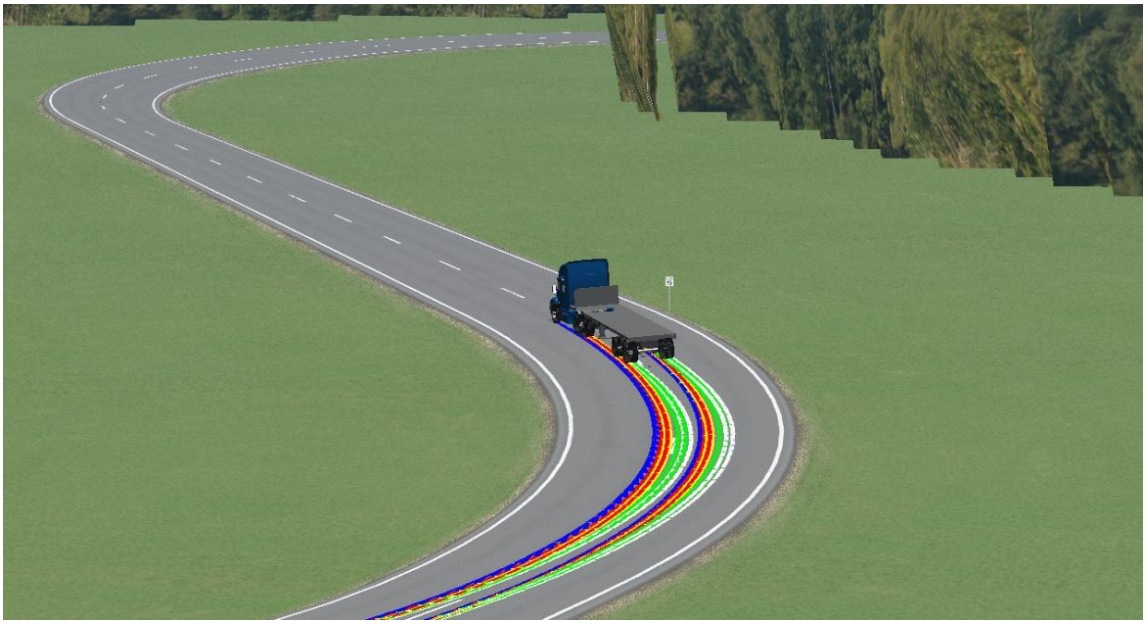

Fig. 1.2: High speed Path-Following Off-Tracking during constant radius turn maneuver

Australian PBS also specifies high speed path-following limits termed as *high speed Path-Following Off-Tracking (PFOT)*. Both types of PFOT are briefly discussed below as a comparison basis:

- *High speed PFOT*, as shown in Fig. 1.2, is the result of centrifugal force. It is observed that a vehicle travels at higher forward speeds, and the rear axle pulls outward from the steering axle path during a turn or lane change maneuver. Excessive high speed PFOT may cause a dangerous accident.

- *Low-speed PFOT*, as shown in Fig. 1.3, is mainly determined by the geometric features of AHVs. In low or moderate speed turns, the rear tires are pulled inward of the curved path. The longer the wheelbase of a unit or the tighter the turn, the higher the PFOT. Some researches on traffic accident prove that PFOT is a crucial problem for safe vehicle operations [22]. The design of pavements, roads, parking lots and trucking yards requires more land areas to ensure the safety operations of AHVs.

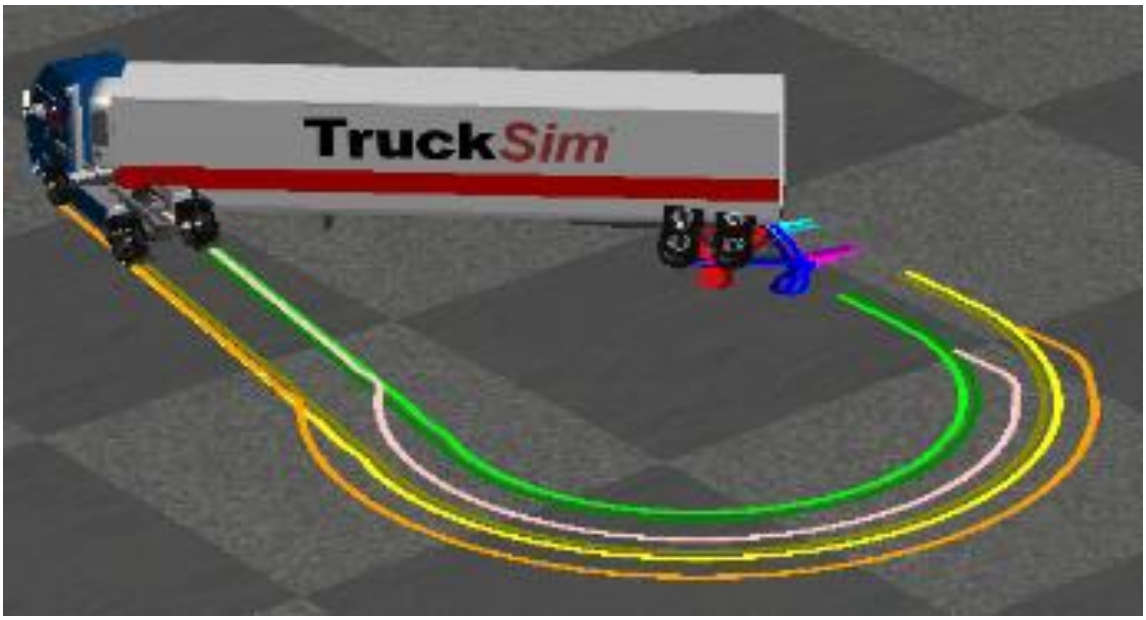

Fig. 1.3: Low speed Path-Following Off-Tracking

Among all these performance measures associated with high-speed AHV safe operations, the RWA ratio is critical. However, at low speeds, the PFOT error becomes the dominating concern. RWA ratio at high speeds and PFOT at low speeds are the main performance measures for stability and maneuverability, respectively. These two

performance measures are conflicting. Thus contradictory design goals may be the most fundamental and important in the design of AHVs. The coordinating of these conflicting design goals will be the main task of this thesis.

1.4 THESIS CONTRIBUTIONS

To solve the contradictory design problem, proposed a variety of passive or active trailer steering (ATS) systems. These studies focused on identifying the effects of either passive or active trailer steering systems using dynamic simulation and analysis. These studies do not address adequately the trade-off relationship between path-following ability at low speeds and stability at high speeds in their design synthesis approaches. In conventional dynamic analysis of active trailer steering (ATS) systems of AHVs, the passive vehicle system is designed first from mechanical viewpoint. Then, the ATS systems are designed and added onto the vehicle already designed. This sequential design approach may not achieve optimal trade-off solutions between the contradictory performance requirements of AHVs [12].

In this thesis, a new design synthesis approach is proposed: with design optimization techniques, the active design variables of ATS systems and passive design variables of trailers can be optimized simultaneously; the ATS controller derived has two operational modes, one for improving lateral stability at high speeds and the other for enhancing path-following at low speeds. To demonstrate the effectiveness of the proposed approach, it is applied to the design of an ATS system for a tractor/full-trailer combination based on

a 3 degree of freedom (DOF) linear yaw plane model. It is expected that the proposed approach can be used for identifying desired design variables and predicting performance envelopes in the early design stages of AHVs with ATS systems. Moreover, an optimal controller for the ATS system is proposed based on the preview information of lateral position deviation of preceding axle centers.

1.5 THESIS ORGANIZATION

In this thesis two different optimization design methods for AHVs are examined and investigated. Chapter 1 serves as an introductory chapter, providing general background information of different performance measures of AHVs. Chapter 2 offers the state-of-the-arts of researches on the design of AHVs with ATS systems. Chapter 3 introduces the relevant vehicle models, basic control technique, and one optimization algorithm. Chapter 4 presents a two design loop (TDL) method for predicting design envelop of AHVs by selecting both active and passive design variables. Chapter 5 describes another design method, called single design loop (SDL), where both active and passive variables are optimized simultaneously. In this chapter the SDL method is also compared with the TDL method. Chapter 6 presents the design of an optimal ATS controller based on the preview information of lateral position deviations of preceding axle center. Chapter 7 concludes the thesis, summarizing its findings and providing suggestions for future work in the field of the current research.

Chapter 2

LITERATURE REVIEW

2.1 INTRODUCTION

This chapter offers a comprehensive literature review of the state-of-the-art of AHVs design. More attention is directed towards the design of ATS system.

The last two decades have witnessed the advances in trying to find solutions to the contradictory design goals of maneuverability at low speeds and lateral stability at high speeds. A variety of passive trailer steering systems have been developed. However, these systems can only improve low-speed maneuverability of AHVs. Recently, a lot of efforts have been focused on the development of active trailer steering systems. Numerical simulations show that active trailer steering system can achieve acceptable levels of RWA and PFOT [29].

2.2 PASSIVE TRAILER STEERING SYSTEMS

Aurell and Edlund examined the influence of the location of passive steered axles on the dynamic stability of a tractor/semi-trailer system [31]. Jujnovich and Cebon compared the performance of various passive trailer steering systems [32]. Results derived from these studies imply that identifying optimal design variables, such as the trailer length, axle

group location and weight distribution etc., can lead to the improvement of both high and low speed performance.

2.2.1 Low-Speed Maneuverability

In order to improve low-speed path-following of AHVs, several passive trailer steering systems, including self-steering, command steering, and pivotal bogie mechanisms, have been developed [25]. It is found that these passive trailer steering systems can improve path-following ability at low speeds. A comparative study of self-steering, command steering, and pivotal bogie systems was conducted by Sanker *et al.* [43]. In their study, the command steering, also called force steering, system is used. These passive systems implement trailer steering based on a geometric relationship with articulation angle or a tire force balance. In this passive steering system, the steering angle of a rear axle is considered as proportional to the articulation angle. The directional dynamics analysis of self-steering and command steering systems of a tractor semi-trailer combination reveals that the Path-Following Off-Tracking (PFOT) is significantly reduced at low speeds. These trailer steering systems also substantially reduce lateral tire forces. As a result, an AHV with passive steering system is more maneuverable, and able to access more of the road network. They reduce tire wear and also decrease the damage of the road surface whilst turning compared to conventional fixed-axle semi-trailer. However, their study also reported that, at low-speed, passive steering system may increase the amount of tail swing.

2.2.2 Poor High-Speed Stability

Although at low-speeds the AHVs, with passive steering systems, exhibit improved performance, at high-speed their stability decreases [1, 28]. Jujnovich and Cebon [32] also reported that the high-speed performance measures, in both Rear-Ward Amplification (RWA) ratio and transient PFOT, are low with passive steering systems. This results support the rules of thumb suggested by Fanchar and Winkler [1] that "what one does to improve low-speed performance is likely to degrade high-speed performance and vice versa". As previously mentioned, articulated heavy vehicles (AHVs) exhibit unstable motion modes at high speeds, including jack-knifing, trailer swing and roll-over [25]. These unstable motion modes may lead to fatal accidents. Thus, at high-speed these passive steering systems might cause serious traffic accidents.

To tackle this problem, it is a common practice that passive trailer steering systems are locked in high-speed operations.

2.3 ACTIVE TRAILER STEERING SYSTEMS

The last two decades have witnessed the advances in trying to find solutions to the contradictory design goals of path-following at low speeds and lateral stability at high speeds. A number of active trailer steering (ATS) systems have also been proposed for reducing Path-Following Off-Tracking (PFOT) at low speeds [29, 30, 49, 50]. In 2003, Wu and Lin [33] studied the dynamic effect of a multi-axle full- trailer with an active steering system using yaw-plane model. The front steering axle of trailer is able to reduce PFOT using a fixed steer ratio. The *steer ratio* is a multiplying factor to tractor steering

angle to determine the trailer axle steering angle. This study also provides an interesting phenomenon that, with the introduction of a multi-axle steering system, the transient PFOT is reduced in a high-speed lane change maneuver. A similar phenomenon is also reported in the results of Rangavajhula's simulations on ATS systems [49]. The yaw plane model of a tractor/full-trailer system was extended to include threefull trailers with steerable trailer axles in their research. They also used a similar steer ratio for steering the trailers and showed that with a given steering input from the tractor driver, the radius of a 90-degree intersection turn was drastically reduced in comparison to non-steerable trailer system. Rangavajhula and Tsao [29] also studied the cost effectiveness of various combinations with different active trailer steering axles. Their study concludes that the ATS system with only the first and second trailer steerable axles is the most cost effective for an AHV with threefull trailers.

2.3.1 RWA Ratio as a Control Criterion

El-Gindy *et al.* used RWA ratio as a control criterion in the design of active yaw controllers for a tractor/full-trailer combination [4]. It is demonstrated that compared with the baseline vehicle, the one with the active trailer yaw controller can reduce the RWA level without significant change of the baseline vehicle trajectory. Rangavajhula and Tsao also used RWA ratio as the control criterion in the design of optimal trailer steering controllers based on the linear quadratic regulator (LQR) technique [29, 30]. Numerical simulations show that active trailer steering systems can achieve acceptable levels of RWA and PFOT. Interestingly, they proved that ATS system improves high-speed

performance also. Their research illustrates that the ATS system not only improves low-speed maneuverability, but also enhanced high-speed stability during a lane change maneuver by reducing Rear-Ward Amplification (RWA) ratio.

2.3.2 Simulation Environments

However, Wu *et al.* [33], and Rangavajhula *et al.* [29, 30, 49, 50] performed the simulation of high-speed single lane change maneuver by considering the forward speed as 55 km/h. The open-loop steering input is a single sinusoidal wave with a 4 second time period. However, the ISO [51] and SAE standards [52] suggest that the forward speed during high speed lane change test should be 88 km/h and the open-loop steering input should be a single sinusoidal wave with a 2.5 second time period. To effectively evaluate the high-speed lateral stability of AHVs, the selected vehicle forward speed of 55 km/h is not reasonable.

Moreover, their research is based on the design criterion: the lower the RWA ratio, the better the high-speed stability of AHVs. However it is argued that RWA ratio of 1.0 is ideal for the trailing units to follow the motion of the tractor in a multi-trailer articulated vehicle. A low RWA ratio, *e.g.* 0.1, may degrade the path-following ability of the vehicle.

To assume safe operating conditions in obstacle avoidance situations on highways, the following performance requirements should be considered: 1) to avoid the obstacle, all vehicle units of the AHV should respond the driver steering input quickly and adequately; and 2) no unit should be allowed to roll-over. If the RWA ratio is much

greater than 1.0, the rear unit will roll-over at a relatively low level of lateral acceleration. However, if the RWA is much less than 1.0, the rear unit will not follow the path of the lead unit around the obstacle.

2.3.3 Passive and Active Steering System Together

To improve compatibility between low-speed PFOT and high-speed RWA, researchers have investigated a variety of potential solutions. It is reported that the location of steered axles and the types of steering mechanism have significant effects on the dynamic stability of a tractor/trailer system [31]. The RWA ratio has been used as a control criterion in the design of active yaw controllers for a tractor/full-trailer combination [4]. Recently, the linear quadratic regulator (LQR) technique has been applied to the controller design of ATS systems for AHVs [29, 30]. The researchers intended to identify the correlation between the RWA ratio and the PFOT value in order to reduce the latter through minimizing the former. Another solution accepted to date is to use a passive and an active trailer steering system [4, 28, 30]. At low speeds, the passive steering systems are employed in order to effectively decrease PFOT values. From medium to high speeds, ATS systems are applied to ensure that AHVs have high stability. This solution provides a good way to coordinate the conflicting design criteria at low and high speeds, but it increases the complexity of trailer configurations since the ‘dual’ steering systems co-exit.

2.4 CONTROLLER DESIGN FOR ATS SYSTEMS

El-Gindy *et al.* used RWA ratio, as a control criterion, in the design of active yaw controllers for a tractor/full-trailer combination [4]. The vehicle under consideration was a six-axle tractor/full trailer combination, which usually exhibits a high level of RWA leading to roll-over during obstacle avoidance maneuvers.

In their research, several control strategies were investigated to improve high-speed stability: active yaw control at the truck CG, active yaw control at the dolly CG, and active yaw control at the trailer CG. They investigated all those control techniques both individually and in combination. The outcome of the active control torque applied to different vehicle units of AHV was examined via an optimal linear quadratic regulator (LQR) approach incorporated with a simplified 4 degrees-of-freedom linear vehicle model. The controller performance index parameters were estimated using an ad-hoc fashion based on acceptable RWA target values. The sensitivity of the controller to tyre cornering stiffness variation, of ± 20 percent of their nominal values, was further investigated. Their simulation results indicated that the RWA could be decreased, when active yaw torque was applied to the dolly, without significant change of the trajectory of uncontrolled vehicle. The controller could be more efficient, if applied to the lead unit or to the rearward unit, in enhancing the dynamic performance and roll stability. The trajectory of the AHV became greatly affected and driving difficulties was also experienced. For active yaw control at the dolly CG, the optimal controller was found to be most sensitive to the cornering stiffness variation of dolly tyre and least sensitive to steering axle from the Rear-Ward Amplification level. They also found that the controller

was greatly sensitive to steering axle parameter variations for path following ability of the vehicle.

Differential breaking is used by Fancher *et al.* [59] to control the lateral stability at high speeds reducing snaking unstable motion modes. Their control strategy of commanding brake pressures to the axle tires was such that yawing of the dolly could steer thefull trailer along with controlling the lateral acceleration. With sinusoidal driver steering input of a 2.5 second period they improved the vehicle high-speed performance by reducing RWA ratio from value of 2.3 to 1.7. In their studies, the desired RWA ratio was 1.0. The Rear-Ward Amplification suppression system should not be on all of the time, as it might cause excessive use of compressed air or cause the brakes to overheat and wear excessively, even if the amount of braking were not slight.

Tanaka [57] used a fuzzy controller to control the backward movement of a tractor/semi-trailer system via a model-based fuzzy control technique. Takagi–Sugeno fuzzy modeling [48] approach was applied to nonlinear dynamic model of AHV. They studied AHVs for low speed jackknife preventive backward path-following issues. A nonlinear dynamic vehicle model was developed based on a Takagi–Sugeno fuzzy model. The idea of parallel distributed compensation was utilized to estimate a fuzzy controller from the Takagi–Sugeno fuzzy model of the vehicle. To ensure the controller stability of their proposed system, they used Lyapunov method. The stability conditions were characterized in terms of linear matrix inequalities since the stability analysis is decreased to a problem of finding a common Lyapunov function for a set of Lyapunov inequalities.

Both their simulation and experimental investigations showed that the designed fuzzy controller effectively achieved the backward movement control of the articulated vehicle. Recently, linear quadratic regulator (LQR) technique was applied to the controller design for ATS systems of multi-trailer articulated heavy vehicles in order to improve both low-speed maneuverability and high-speed stability [30, 29]. Numerical simulations show that ATS systems can achieve acceptable levels of RWA ratio and PFOT. However, in the LQR controller construction, the design criteria were not clearly explained and justified.

It was indicated that the trailer tires could be steered through an angle proportional to the single-point path preview lateral position error and results illustrated that the preview controller provided a moderate tracking capability [67]. A path-following steering controller in the discrete time domain was developed for an ATS system of a semi-trailer for improving both maneuverability at low-speeds and stability at high-speeds [69]. The controller steered the semi-trailer tires and the trailer rear end followed the trajectory of the 5^{th} wheel at all speeds. However, the applicability of the controller to afull trailer has not been addressed.

2.5 LIMITATIOINS OF EXISTING DESIGN AND ANALYSIS METHODS

All the above studies focused on identifying the effects of either passive or active trailer steering systems on the contradictory design goals based on dynamic simulation and analysis. However, these studies have not addressed the trade-off relationship between

path-following at low speeds and later stability at high speeds using design synthesis approaches. In these dynamic analyses of active trailer steering (ATS) systems of AHVs, it was assumed that the passive vehicle system was designed first and then the ATS systems developed were added onto the vehicle originally designed from a purely mechanical viewpoint. This sequential design approach may not achieve optimal trade-off solutions between the contradictory performance requirements of AHVs [23].

Past studies mainly focused on investigating the effects of key design variables and influence of either passive or active trailer steering systems on the contradictory design goals based on dynamic simulation and analysis. This is a trial and error approach, where designers iteratively change the values of design variables and reanalyze until acceptable performance criteria are achieved. For example, in the LQR controller design for ATS systems, this approach is commonly used to determine desired weighting factors for the cost function. This manual design process is tedious and time-consuming. With the stringent conflicting performance requirements, the design of AHVs should switch from pure simulation analysis to extensive design synthesis.

To address the limitations of the existing design and analysis approaches, the thesis will investigate innovative methods for the design of AHVs with ATS systems.

Chapter 3

VEHICLE MODELING AND DESIGN TOOLS

3.1 INTRODUCTION

This thesis will focus on addressing design synthesis methods for AHVs with ATS systems. To examine and evaluate these methods, they will be applied to the design of a tractor/full-trailer system with ATS system. In this chapter, the relevant vehicle models, the basic control technique, and one optimization algorithm are briefly introduced.

3.2 VEHICLE MODELING

To predict vehicle dynamic behaviors, two vehicle models, namely Model-1 and Model-2 are introduced in the design synthesis of AHVs with ATS systems.

3.2.1 Model-1

In order to evaluate the high-speed lateral stability and low-speed path-following of the tractor/full-trailer combination, the 3-DOF linear yaw plane model [33, 34] is outlined in this section.

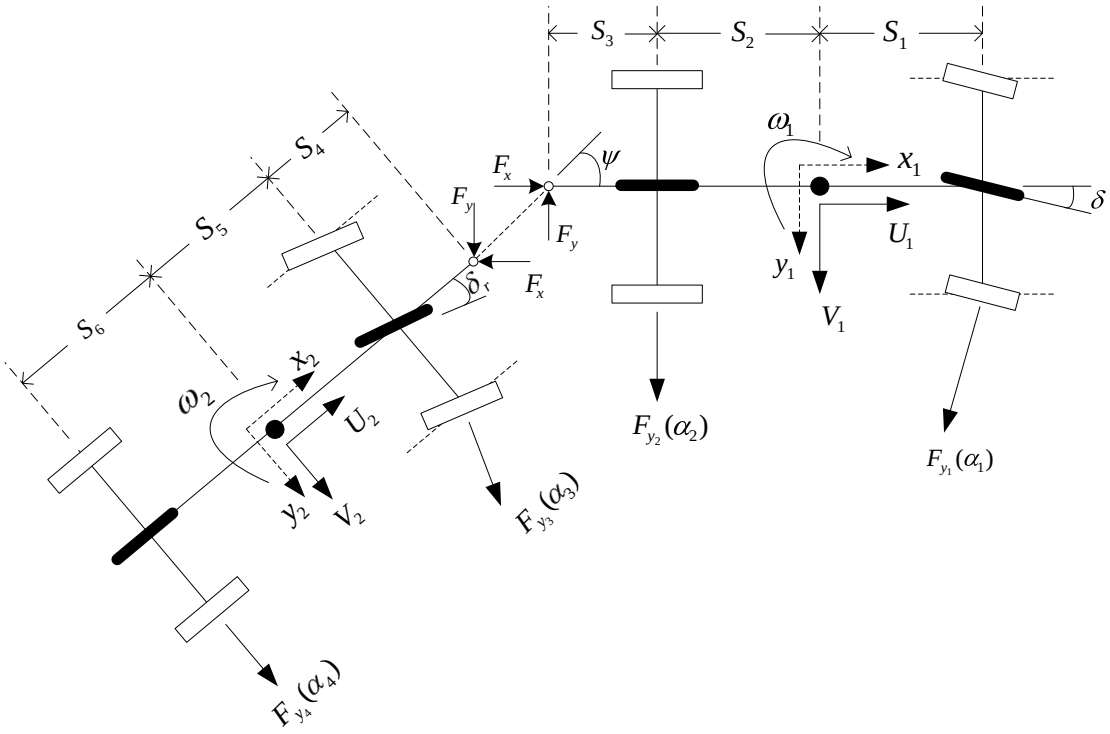

Fig. 3.1: Schematic diagram showing degrees of freedom and system parameters of vehicle Model-1

The articulated vehicle consists of a tractor/full-trailer, which are connected by a hinge pin. As shown in Fig. 3.1, the system is telescoped laterally and each axle set is represented by one tire. Based on the body fixed coordinate systems $x_1 - y_1$ and $x_2 - y_2$ for the tractor and trailer, respectively, the governing equations of the system can be derived. The motions considered are tractor lateral velocity V_1, tractor yaw rate ω_1 and articulation angle ψ between the tractor and trailer. In this model, aerodynamic forces, rolling and pitching motions, and longitudinal forces between tire and road are ignored. From Newton's laws of dynamics, the equations of motion for the tractor are written as

$$m_1\left(\dot{U}_1 - V_1\omega_1\right) = F_x - F_{y1}\sin\delta \tag{3.1a}$$

$$m_1\left(\dot{V}_1 + U_1\omega_1\right) = -F_y + F_{y1}(\alpha_1)\cos\delta + F_{y2}(\alpha_2) \tag{3.1b}$$

$$I_1\dot{\omega}_1 = F_y d + F_{y1}(\alpha_1)S_1\cos\delta - F_{y2}(\alpha_2)S_2 \tag{3.1c}$$

and the equations of motion for the trailer are cast as

$$m_2\left(\dot{U}_2 - V_2\omega_2\right) = -F_{y3}(\alpha_3)\sin\delta_r - F_x\cos\psi - F_y\sin\psi \tag{3.2a}$$

$$m_2\left(\dot{V}_2 + U_2\omega_2\right) = F_{y4}(\alpha_4) + F_{y3}(\alpha_3)\cos\delta_r - F_x\sin\psi + F_y\cos\psi \tag{3.2b}$$

$$I_2\dot{\omega}_2 = -F_{y4}(\alpha_4)S_6 + F_{y3}(\alpha_3)S_5\cos\delta_r + F_y e\cos\psi - F_x e\sin\psi \tag{3.2c}$$

where the notation is given in Appendix A.

To derive the simplified vehicle model, the following assumptions have been made: 1) the forward speed U_1 remains constant; 2) the tractor steering angle δ is small; 3) the articulation angle ψ is small; 4) all products of variables are ignored; 5) the lateral tire force $F_{yi}(\alpha_i)$ is linear functions of sideslip angle α_i, $i = 1, 2, \ldots, 4$. The velocities of the pin using either of the coordinate systems should be compatible. Eliminating the coupling reaction forces F_x and F_y from equations (3.1) and (3.2) leads to the following 3-DOF linear yaw plane model expressed in the state space form as

$$\dot{\mathbf{x}} = \mathbf{A}\mathbf{x} + \mathbf{B}\mathbf{u} + \mathbf{C_1}\delta \tag{3.3}$$

where the matrices **A**, **B**, and $\mathbf{C_1}$ are provided in Appendix B. The state vector **x** and control vector **u** are expressed as

$$\mathbf{x} = [V_1 \quad \omega_1 \quad \dot{\psi} \quad \psi]^T \tag{3.4}$$

and

$$\mathbf{u} = [\delta_r] \tag{3.5}$$

Note that **u** is the control vector related to the trailer front axle tire steering angle.

3.2.2 Model-2

As shown in Figs. 3.1 and 3.2, the only difference between Model-1 and Model-2 is the rear axle of the trailer. In the case of Model-1, the tire on this axle is non-steerable, while in the case of Model-2, the tire on this axle is steerable. For Model-2, the equations of motion for the trailer are listed as follows,

$$m_1\left(\dot{U}_1 - V_1\omega_1\right) = F_x - F_{y1}\sin\delta \tag{3.6a}$$

$$m_1\left(\dot{V}_1 + U_1\omega_1\right) = -F_y + F_{y1}(\alpha_1)\cos\delta + F_{y2}(\alpha_2) \tag{3.6b}$$

$$I_1\dot{\omega}_1 = F_y d + F_{y1}(\alpha_1)S_1\cos\delta - F_{y2}(\alpha_2)S_2 \tag{3.6c}$$

and the equations of motion for the trailer are cast as

$$m_2\left(\dot{U}_2 - V_2\omega_2\right) = -F_{y3}(\alpha_3)\sin\delta_f - F_{y4}(\alpha_4)\sin\delta_r - F_x\cos\psi - F_y\sin\psi \tag{3.7a}$$

$$m_2\left(\dot{V}_2 + U_2\omega_2\right) = F_{y3}(\alpha_3)\cos\delta_f + F_{y4}(\alpha_4)\cos\delta_r - F_x\sin\psi + F_y\cos\psi \tag{3.7b}$$

$$I_2\dot{\omega}_2 = F_{y3}(\alpha_3)S_5\cos\delta_f - F_{y4}(\alpha_4)S_6\cos\delta_r + F_y e\cos\psi - F_x e\sin\psi \tag{3.7c}$$

The state space form to equations (3.6) and (3.7) are expressed as

$$\dot{\mathbf{x}}(t) = \mathbf{A}\mathbf{x}(t) + \mathbf{B}\mathbf{u}(t) + \mathbf{C_2}\delta(t) \tag{3.8}$$

where the matrices **A**, **B**, and $\mathbf{C_2}$ are provided in Appendix B. The state and control variable vectors **x** and **u** are expressed in equations (3.4) and (3.5) respectively.

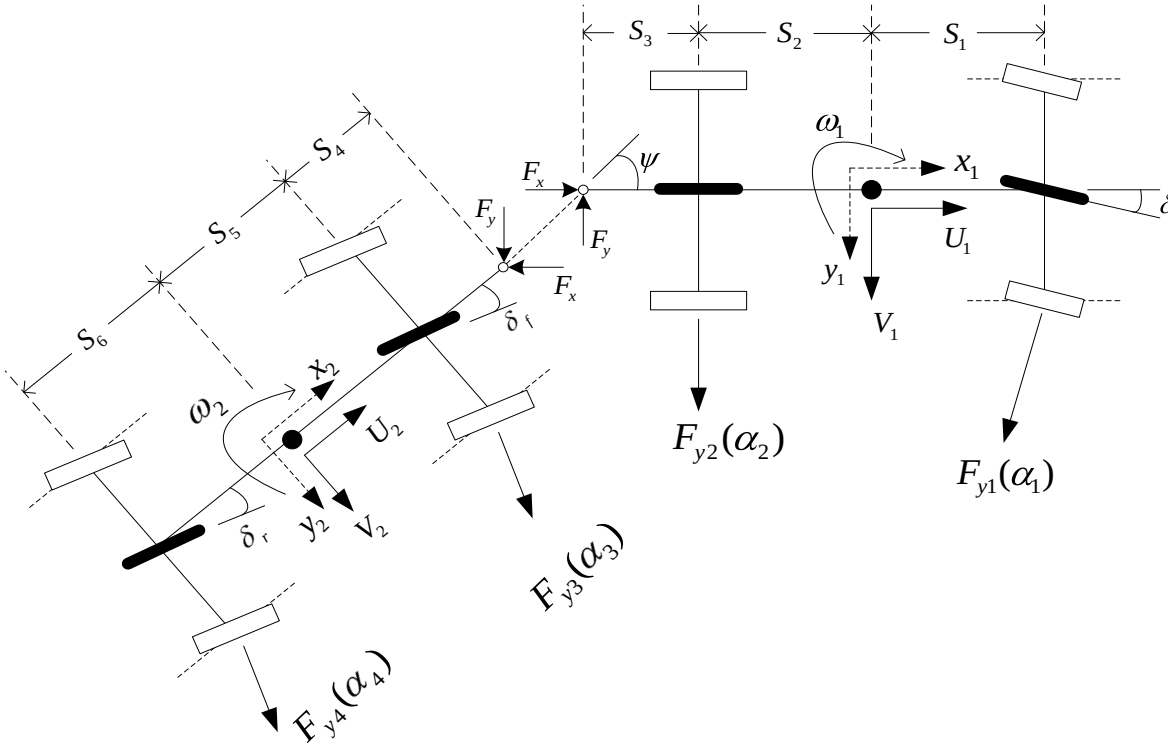

Fig. 3.2: Schematic diagram showing degrees of freedom and system parameters of vehicle Model-2

Note that **u** is the control variable vector related to the trailer front and rear axle tire steering angles. For simplicity it is assumed that forward velocity at the tractor CG $U_1$and that at the trailer CG U_2 are constant and both take the same value.

3.3 TEST MENEUVERS

To evaluate AHVs' performance levels in high-speed RWA ratio and low-speed Path-Path-Following Off-Tracking (PFOT), two types of simulations have been used: open-loop and close loop simulation.

3.3.1 Open-Loop Simulation

The first type is based on an open-loop control approach with specified steer inputs, including pulse and step steer inputs. These simulations require the precise application of a predetermined steer sequence and the resultant vehicle responses are observed. To assess the RWA and path-following levels, respectively, one-period sinusoidal steer inputs [29-31, 33] and step steer inputs [29, 30] have been used accordingly.

- ***High-Speed Case***

A single lane change maneuver is simulated for determining the high-speed RWA ratio. In the simulation, the vehicle is traveling at the speed of 88 km/h along a straight path and a sudden lane change is conducted. The lateral displacement of the vehicle in the lane change is 3.7 m. The steering input, in radians, for this maneuver takes a single sinusoidal wave as

$$\delta(t) = A \sin\left(\frac{2\pi}{T} t\right) \tag{3.9}$$

where the period T is 2.5 seconds and the value of amplitude A is selected in such a way that the vehicle is able to complete the single lane change.

- ***Low-Speed Case***

The maneuver emulated for measuring low-speed Path-Following Off-Tracking (PFOT) is based on a step steer simulation, which is similar to the 360-degree roundabout defined in the United Kingdom's Road Vehicles Regulation [32]. In this near zero-speed path-following task, once the transients have settled after the initial application of steer, the vehicle will enter a steady turn and follow a circular path on a constant radius. As shown in Fig. 3.3(a), in the simulation, the centre of tractor front axles is required to travel along a section of straight path first and then approach to a circular arc with a radius of 11.25 m. The vehicle forward speed is less than 4 km/h. The step steer input follows the schedule illustrated in Fig. 3.3(b). The maximum steer angle δ_{max} is determined in such a way that the centre of tractor front axle follows a circular path with its radius approaching 11.25m.

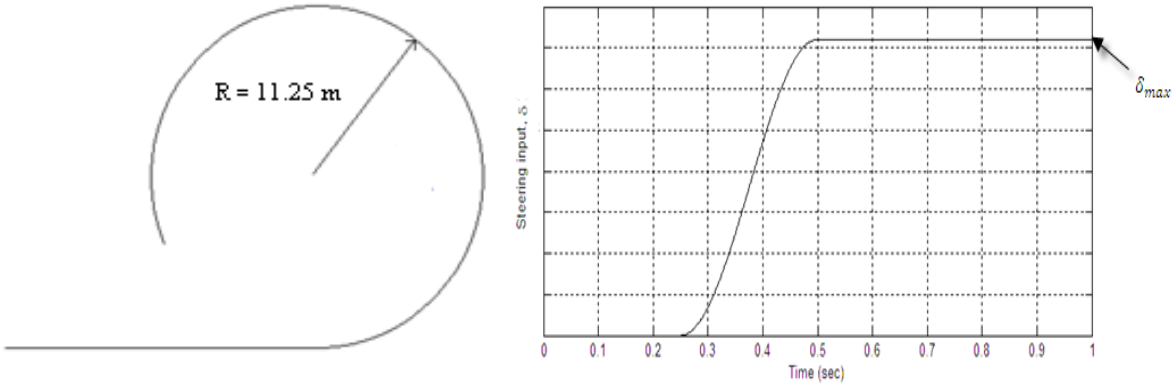

(a) (b)

Fig. 3.3: (a) layout of circle path-following test course; (b) step steer input for circle path-following [26]

In open-loop tests, specific steering inputs are predefined and they are not dependent on the response of the vehicle. These tests can be conducted with high repeatability and they

are used for the purpose of characterizing only vehicle responses. Open-loop tests ignore human/vehicle interactions and thus only provide limited useful information.

3.3.2 Closed-Loop Simulation

The second type is essentially a closed-loop steer control process. In these simulations, a driver model is introduced and the vehicle model follows a well-defined path under the control of the driver model. During the process, the combined driver/vehicle models' responses are observed. To determine the RWA ratio of AHVs with semi-trailer steering systems based on the lane change maneuver recommended by SAE [35], a driver model has been used [32].

In closed-loop tests, a desired vehicle motion or trajectory is achieved by continuously monitoring vehicle response and adjusting steering actions accordingly. In a closed-loop test, the driver is considered as an integral part of the system to the extent that the mathematical model of the entire system involves a driver model [32]. Because of the cost and safety concerns, it may not be practical to perform field testing. Simulation assessment thus may be more practical in certain situations. Moreover, computer simulations provide an efficient means to analyze the interaction between the human driver and the vehicle, even before a vehicle or its subsystems are produced. In past studies on ATS systems for AHVs, only the open-loop tests were simulated to evaluate the vehicle's performance measures in RWA ratio and PFOT value [12, 29, 30, 33]. Obviously, these studies cannot provide sufficient information regarding the interaction between the human driver and the ATS systems in computer-based vehicle design processes. Thus, in the current research, to demonstrate the efficacy of the

proposed design synthesis approach, a simplified driver model has been generated and the closed-loop tests have been simulated for evaluating vehicles' directional performance.

3.4 LINEAR QUADRATIC REGULATOR TECHNIQUE

In this thesis, the controllers designed for ATS systems are mainly based on the linear quadratic regulator (LQR) technique.

The LQR is introduced by Kalman in Ref. [63] and [64]. The infinite horizon LQR problem considers the linear time-invariant plant

$$\dot{x}(t) = Ax(t) + Bu(t) \tag{3.10}$$

where $A \in \mathbb{R}^{n\times n}$ is the state matrix, $B \in \mathbb{R}^{n\times m}$ is the input matrix, $x \in \mathbb{R}^{n\times 1}$ is the state vector, and $u \in \mathbb{R}^{m\times 1}$ is the control vector. The time-invariant quadratic cost functional

$$J = \int_0^\infty [x^T(t)Qx(t) + u^T(t)Ru(t)]dt \tag{3.11}$$

with

$$Q = Q^T \geq 0 \quad \text{and} \quad R = R^T > 0 \tag{3.12}$$

and the desired feedback controls of the form

$$u(t) = \mu(x(t)) \tag{3.13}$$

The sufficient condition for the optimality is given by

$$\frac{\partial V^T}{\partial x}\left(Ax + B\mu^*(x)\right) + x^T Q x + \left(\mu^*(x)\right)^T R\mu^*(x) = 0 \tag{3.14}$$

and for arbitrary admissible $\mu\left(x(t)\right)$

$$\frac{\partial V^T}{\partial x}(Ax + B\mu) + x^T Q x + \mu^T R\mu \geq 0 \tag{3.15}$$

It is easy to see that (3.13) and (3.14) are satisfied by

$$V(x) = x^T P x \tag{3.16}$$

and

$$\mu^*(x) = -R^{-1}B^T P x \tag{3.17}$$

provided

$$A^T P + PA + Q - PBR^{-1}B^T P = 0 \tag{3.18}$$

The above equation (3.18) is known as the Algebraic Ricatti Equation (ARE).

3.5 GENETIC ALGORITHMS

As will be discussed in Chapter 4 and 5, a genetic algorithm (GA) will be the basic optimal search algorithm used in the design synthesis methods. Thus, the characteristics of GAs are briefly introduced.

Evolutionary computation or evolutionary computing represents a broad area that covers a family of adaptive search population based methods that can be applied to the optimization of both discrete and continuous mappings. They have different features from the typical single-point-based optimization techniques, such as gradient search techniques

and other directed search techniques [60], by the fact that their search mode is executed based upon multiple positions in the search space rather than upon a single position. Genetic algorithm is one of the very attractive methods of this computational paradigm [61].

3.5.1 Genetic Algorithm and Optimization

The GA search optimization algorithm was formulated first by Holland [62]. This is a derivative-free based technique which makes it applicable to smooth functions, simply continuous functions, or even discontinuous functions. This efficient search technique, especially to achieve global optima, is based on biologic evolution and on the survival of the fittest principal. This algorithm evaluates the function at a set of points in the function's variable space, usually chosen randomly within their allocated search range. This aspect makes them good candidates for solving global optimization problems and makes them less vulnerable to local optima. The solution is reached based on iterative search procedure, and as such mimics to a certain extent the evolution process of biological entities. To understand this genetic algorithm properly, two most important terms are defined: the genotype of a population and its fitness value.

3.5.2 Genotype

In *artificial evolution* the "data" of the system considered is approximated as a living creatures in the framework of *natural evolution*. In nature, each individual represents a potential solution to the challenge of survival, while in GA a set of potential solutions are considered. This collection is termed as a *population* and each single solution is called an

individual. Each individual in nature has a form which is determined by its DNA and its set of genetic train is referred to as a *genotype*. The term genotype, in GA, represents the encoding of a problem solution denoted by an individual. Many individuals in a population may have the same or similar genotypes. An individual's genotype is termed, in GA, as its *chromosome*. Strings, also called bits or characters, are normally used to represent genotype in GA. Each single unit of genetic information is referred as *gene* which is determined by each element of the string.

In nature, these genes control various traits in the individual. In humans, genes determine, for example, eye and hair colour and also numerous other characteristics. In a genetic algorithm, a solution encoding also may make use of several interacting genes. Each gene consists of one or more possible values, called *alleles*. If a specific gene represents eye color, each allele represents each color for that gene: brown, black, blue etc. For a particular gene, the number of alleles is fixed in nature, while it is determined by the encoding of solutions in artificial evaluation. The number of gene in a genotype is fixed in genetic algorithm.

3.5.3 Fitness Function

The *fitness* of a creature in nature refers to its ability to survive in its environment. In GA, it represents the *value* or *goodness* of a particular solution. A "fitter" creature is able to find food and shelter better than another. Similarly, the fitness of an individual solution leads the concept of *fitness function*, also called objective function. An objective function denotes a genotype as its parameter and gives usually a real valued outcome that refers to

the *fitness* or *goodness* of the solution. The choice of this objective function is very crucial.

3.5.4 Genetic Algorithm Operators

The technique, a composition of a population changes, is the most important feature of an evolutionary algorithm. Three major forces, in nature, are: *natural selection*, *mating*, and *mutation*. In GA, the corresponding forces are: *selection*, *crossover,* and *mutation*. They are known as genetic operators, and act on individuals, sets of individuals, populations, and genes.

3.5.4.1 Selection

With this procedure an individual is selected that take part in reproduction procedure to give birth to the next generation. Selection operators typically serve to eliminate weaklings from a population, or to select strong individuals for reproduction. These stochastic selection operators probabilistically select good solutions, and eliminate bad ones based on the evaluation given to them by the objective function. The elitist model is considered as a part of several heuristics where a number of populations are chosen for further processing. The ranking model of this process ranks each member of population depending on its fitness value. The roulette tire procedure assigns a probability p_i to each individual i for reproduction. Then the cumulative probability $c_i = \sum_{j=1} p_i$ is determined for each i. If c_i becomes greater than a random number n, corresponding individual is selected.

3.5.4.2 Crossover

Crossover procedure in GA corresponds to the natural phenomenon of mating. However, it refers most specifically the *genetic recombination*, where the genes of two parents are combined randomly to form the genotype of a child. This process involves randomness to select a set of genes from each parent to form genotype of the child. Most common procedure of this crossover operation is to choose a number of points, each for simple crossing, in the binary strings of the two parents to create the offspring by swapping parents' gene sequences around these points. Crossover operation, in this way, generates new combinations of genes, and therefore new combinations of traits.

3.5.4.3 Mutation

Mutation operation can initiate completely new alleles into a population. While crossover and selection serve to explore variants of existing solutions eliminating bad ones, the mutation operation creates completely new solution. In nature, mutations refer to random alterations in genetic material resulting from chemical or radioactive influences, or from mistake made during replication or recombination. In genetic algorithm, mutation operators select genes in an individual at random and change the allele. Generally alleles are changed in a random manner, simply selecting a different allele from those available from that gene. The mutation is implemented by flipping one or more digits of a sting starting from a randomly chosen order.

Chapter 4

TWO DESIGN LOOP METHOD FOR THE DESIGN OF AHVS WITH ATS SYSTEM

4.1 INTRODUCTION

This chapter presents Two Design Loop (TDL) approach, called Two Design Loop (TDL) method, for active trailer steering (ATS) systems of articulated heavy vehicles (AHVs). As mentioned before, of all contradictory design goals of AHVs, two of them, i.e. path-following at low speeds and lateral stability at high speeds, may be the most fundamental and important, which have been bothering vehicle designers and researchers. To tackle this problem, the TDL is proposed: with design optimization techniques, the active design variables of ATS systems and passive design variables of trailers can be optimized simultaneously; the ATS controller derived from this approach has two operational modes, one for improving lateral stability at high speeds and the other for enhancing path-following at low speeds. To demonstrate the effectiveness of the proposed approach, it is applied to the design of an ATS system for an AHV with a tractor/full-trailer.

The rest of this chapter is organized as follows. The vehicle model used is mentioned and the maneuvers emulated are presented in Section 4.2, to evaluate the AHV performance in the lateral stability at high speeds and path-following at low speeds. The

design of the LQR controller for ATS systems is introduced in Section 4.3. The proposed design synthesis approach is presented in Section 4.4. Section 4.5 compares the design results derived from the proposed approach against those based on the baseline vehicle system without ATS systems. Finally, conclusions are drawn in Section 4.6.

4.2 VEHICLE SYSTEM MODELS

4.2.1 Vehicle Model

To examine and evaluate the proposed TDL method, it is applied to the design of the tractor/full-trailer system. The 3-DOF linear vehicle model, i.e. Model-1 introduced in Subsection 3.2.1, will be used to predict the dynamic performance measures of the tractor/full-trailer system.

4.2.2 Maneuver Emulated

The proposed design synthesis approach, to be described in section 4.4, is based on a genetic algorithm, which requires extensive fitness function evaluations. This may lead to poor computation efficiency of the design approach. In the simulations based on the closed-loop steer control, the introduction of driver model will greatly increase computation time. If the driver model is introduced in the design approach, it will further degrade the computation efficiency. Thus, in the current research, the simulations based on the open-loop steer control are utilized to identify the high-speed and low-speed performance measures, as discussed in Section 3.3.

4.3 OPTIMAL CONTROL DESIGN

In Model-1 shown in Fig. 3.1, the front axle of the full trailer is steerable and the steering angle δ_r is determined by the optimal controller based on linear quadratic regulator (LQR) theory [37]. The design criterion of the controller is to minimize the tractor/full-trailer system's RWA ratio at high speeds and PFOT at low speeds. The LQR controller design is an optimization problem: minimize the performance index

$$J = \int_0^\infty \left[q_1 \left(\dot{V}_1 + U_1 \omega_1 \right)^2 + q_2 \left(\dot{V}_2 + U_2 \omega_2 \right)^2 + q_3 (\delta_r)^2 \right] dt \qquad (4.1)$$

subject to equation (3.3). By solving the algebraic Ricatti equation, the solution of the optimization problem is the control vector of the form

$$\mathbf{u} = -\mathbf{K}\mathbf{x} \qquad (4.2)$$

where **K** is the control gain matrix with a dimension of 1×4, **x** and **u** are respectively the state and control variable vectors defined by equations (3.4) and (3.5), respectively. In equation (4.1), q_1, q_2 and q_3 are weighting factors that impose penalties upon the magnitude and durations of the lateral acceleration of the tractor at the centre of gravity (CG), $\dot{V}_1 + U_1\omega_1$, the lateral acceleration of the trailer at CG, $\dot{V}_2 + U_2\omega_2$, and the active steering angle, δ_r, respectively. Note that the third term on the right side of equation (4.1) represents the energy consumption of the active trailer steering system.

4.4 PROPOSED TSD METHOD

In this section, an optimization method for determining the LQR controller parameters is introduced. Then, the proposed TSD method is described.

4.4.1 Method for Determining Controller Weighting Factors

With the LQR controller structure designed in section 4.3, the next step is to determine the controller parameters, i.e. the weighting factor vector $[q_1 \quad q_2 \quad q_3]$ as shown in equation (4.1). After this vector is determined, the control gain matrix **K** indicated in equation (4.2) can be achieved following the procedure described in the previous section. To identify the weighting factor vector, trial and error approaches are commonly used and this is a time-consuming and tedious process [23]. To facilitate the identification of the controller parameters, an optimization method is proposed in the current research. In this subsection, this method is explained through the determination of the weight factors for the controller of the active trailer steering system.

The LQR controller has two operational control modes, i.e. high-speed RWA control mode and low-speed PFOT control mode. The design objective of the RWA control mode is to minimize the RWA ratio in the single lane change maneuver described in subsection 4.2.2. The design criterion of the PFOT control mode is to minimize the PFOT in the circle path-following maneuver.

For the RWA control mode design, the performance index corresponding to that indicated in equation (4.2) takes the following form

$$J_{RWA} = \int_0^{\infty} \left[q_{RWA1}\left(\dot{V}_1 + U_1\omega_1\right)^2 + q_{RWA2}\left(\dot{V}_2 + U_2\omega_2\right)^2 + q_{RWA3}(\delta_r)^2 \right] dt \qquad (4.3)$$

Fig. 4.1 shows the procedure to determine the vector $[q_{RWA1} \quad q_{RWA2} \quad q_{RWA3}]$.The genetic algorithm (GA) [39] sends the randomly selected weighting factor vector to the 3-DOF vehicle model and LQR controller constructed in Matlab. Based on the given weighting factor vector, the controller is updated and corresponding simulation is performed. Then a data processor calculates the performance measure of RWA for the single lane change maneuver based on the simulation results. This set of calculated RWA ratio is used as fitness function values. At this point, if the convergence criteria are satisfied, the optimization terminates. Otherwise, the fitness function values are sent back to the GA. Based on the returned fitness values, the GA produces the next generation of design variable sets using genetic operators, e.g. selection, crossover, and mutation. This procedure repeats until the optimized weighting factor vector is found.

Following the same procedure shown in Fig. 4.1, the weighting factor vector for the low-speed PFOT mode, $[q_{OFF1} \quad q_{OFF2} \quad q_{OFF3}]$, can also be determined.

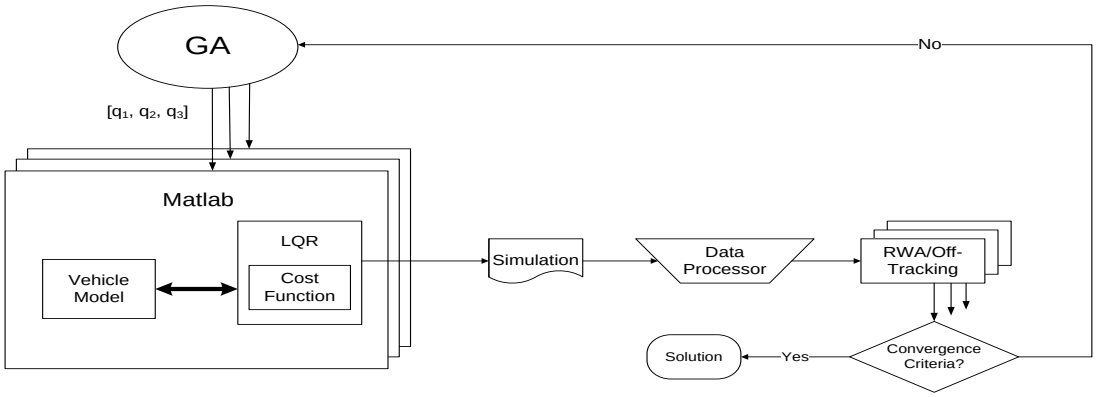

Fig. 4.1: The optimization method for determining LQR controller weighting factors

4.4.2 Proposed Integrated Design Method

For the purpose of simplicity, the proposed design method is described through the design optimization of the active trailer steering system for the tractor/full-trailer combination.

As introduced in the above subsection, the RWA and PFOT modes of the controller are designed independently and the vehicle system parameters (i.e. the passive design variables including vehicle geometry and inertia parameters) take their nominal values. In order to improve the overall performance of the vehicle system, in the following design synthesis, the two control modes are integrated and the passive design variables **X** are optimized. Since the control gain matrix **K** (*i.e.* the active design variables) for each of the two control modes is dependent on **X**, through the design synthesis, the passive and active design variables are optimized simultaneously.

The following utility function is used as the objective function for the design optimization.

$$obj = \frac{1}{\rho_{rwa}} \times F_{rwa}(\mathbf{X}) + \frac{1}{\rho_{off}} \times F_{off}(\mathbf{X}) \tag{4.4}$$

where ρ_{rwa} and ρ_{off} are the performance measures when **X** take their nominal values. These performance measures are achieved using the numerical simulations based on the high-speed single lane change maneuver and the low-speed circle path-following maneuver, respectively. $F_{rwa}(\mathbf{X})$ and $F_{off}(\mathbf{X})$ are the corresponding performance measures with the current design variable set **X**.

This design synthesis is implemented as shown in Fig. 4.2. First, a population of n sets of design variables is randomly selected by the GA; the corresponding sets of design variables are sent forward in parallel to the Matlab platform, where with a given set of design variables **X**, the vehicle system model and LQR controller are updated. Then, the vehicle model simulates to travel in both the high-speed single lane change maneuver and the low-speed circle path-following maneuver, respectively. In these two maneuvers, the LQR controller operates in its high-speed RWA control mode and low-speed PFOT control mode, accordingly. The corresponding data processor determines the resulting performance measure, RWA representing $F_{rwa}(\mathbf{X})$ and PFOT denoting $F_{off}(\mathbf{X})$. These performance measures are sent to the utility function shown in equation (4.4). With this utility function, the resulting fitness value vector $[obj_1 \quad obj_2 \quad ... \quad obj_n]$ can be achieved. At this point, if the convergence criteria are satisfied, the calculation stops;

otherwise, this vector is sent back to the GA. Based on the returned fitness values corresponding to the given sets of design variables, the GA produces the next generation of design variable sets using selection, crossover, and mutation operators. This procedure repeats until the optimized variable set is found.

4.5 RESULT AND DISCUSSION

In this section, the simulation results derived from the following cases are presented and discussed: 1) baseline case, where the design variables **X** take their nominal values and the vehicle has no active trailer steering system; 2) control case, where the design variables **X** and control gain matrices **K** take their nominal values; 3) optimal case, where the design variables **X** and control gain matrices **K** take their optimized values.

4.5.1 Simulation Results of Baseline Case

In the case of numerical simulations for the baseline vehicle with non-steerable trailer axles, the vehicle system parameters take their nominal values listed in Table B1 of Appendix B. The simulation results for the lane change maneuver are shown in Fig. 4.3.

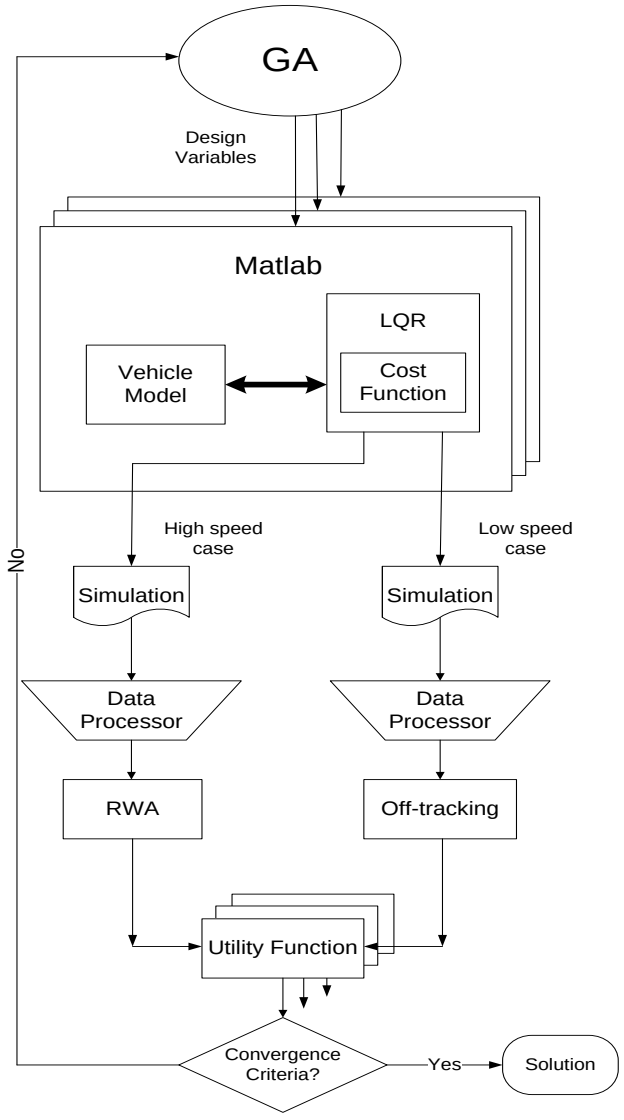

Fig. 4.2: Schematic representation of the proposed design synthesis approach

As shown in equation (3.9), the amplitude of sinusoid steer input, *A*, takes the value of 0.0113. From Fig. 4.3(a), it can be seen that compared with the 2.5 second time period of the sinusoid steer input, the vehicle takes a longer time (around 7 seconds) to reach a steady state. This indicates that the vehicle system is stable, but external perturbations

will take a long time to decay. The RWA ratio is 1.2024. Fig. 4.3(a) shows the trajectory of tractor front axle centre and that of trailer rear axle centre. It is observed that before the trailer reaches the steady state, there is a small overshoot.

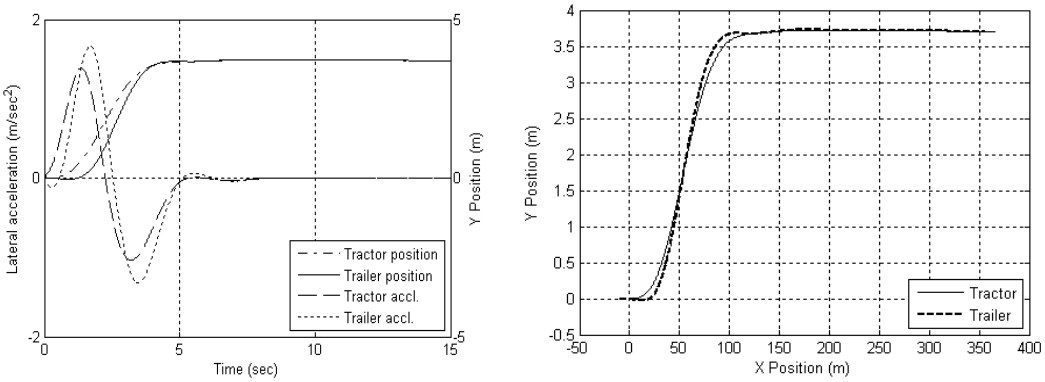

(a) (b)

Fig. 4.3: Baseline case in lane change maneuver (the amplitude of sinusoid steer input, A, taking the value of 0.0113): (a) lateral accelerations at tractor and trailer CG versus time and lateral displacement of tractor front axle centre and that of trailer rear axle center versus time; (b) trajectory of tractor front axle center and that of trailer rear axle

Fig. 4.4 shows the trajectory of the tractor front axle centre and that of the trailer rear axle centre when the vehicle travels in low-speed circle path-following maneuver. The PFOT of the vehicle when traveling in this maneuver indicates the vehicle's ability to negotiate roundabouts. For the baseline vehicle, with the step steer input of $\delta_{max} = 0.072\pi$ the PFOT is 1.0875 m.

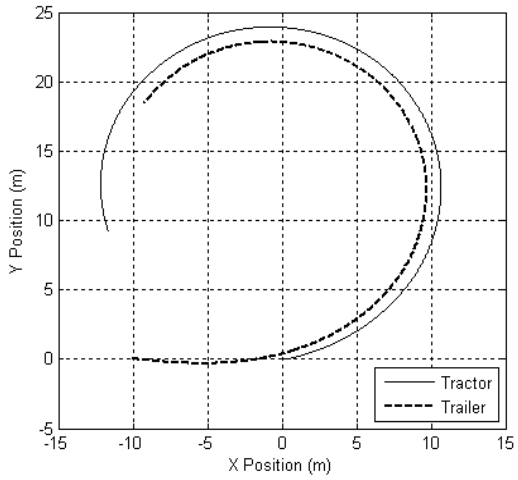

Fig. 4.4: Baseline case in low-speed circle path-following maneuver (with a step steer input of $\delta_{max} = 0.072\pi$): trajectory of tractor front axle centre and that of trailer rear axle centre axle center

4.5.2 Simulation Results of Control Case

To design the LQR controller, the weighting factor vectors for the RWA and PFOT control modes are determined using the method shown in Fig. 4.1. To determine these vectors, the vehicle parameters take their nominal values listed in Table B1 of Appendix B. The relevant controller parameters and performance measures of the two control modes are listed in Table 4.1.

Fig. 4.5 shows the relationships of RWA ratio and PFOT value versus the corresponding weighting factors. Note that in these 3 dimensional curves, only two weighting factors are variables, the third one is fixed and takes the value of 1. In the case of PFOT control mode, the purpose is to identify a weighting factor vector that minimizes the PFOT measured in the low-speed circle path-following maneuver. In the case of RWA control mode, the aim is to find a weighting factor vector that minimizes the RWA

ratio observed in the high-speed lane change maneuver. As shown in Figs. 4.5(a), 4.5(b) and 4.5(c), the

Table 4.1: Resulting controller parameters and performance measures of the two control modes

	RWA control mode	**PFOT control mode**
Weighting factor vector	$[10^{9.9419} \quad 10^{-3.1656} \quad 10^{-0.7019}]$	$[10^{-1.5108} \quad 10^{-1.2863} \quad 10^{1.4776}]$
Control gain matrix	$[0.0995 \quad -1.1379 \quad -0.0334 \quad -0.5156]$	$[-0.7043 \quad 3.6369 \quad -2.5142 \quad -0.5098]$
RWA ratio (high-speed)	0.8296[#]	0.9782 *
PFOT /m (low-speed)	2.2026 **	0.8497[##]

* To operate the PFOT control mode in the high-speed lane change maneuver, the vehicle forward speed dependent control gain matrix **K** takes the value of [0.0132 -0.3793 0.0229 -0.6730].

** To operate the RWA control mode in low-speed circle path-following maneuver, the control gain matrix **K** takes the value of [-5.4182 0.1196 -0.7351 -0.5156].

[#] This RWA ratio value is the performance measure ρ_{rwa} shown in equation (4.4).

[##] This PFOT value is the performance measure ρ_{off} shown in equation (4.4).

performance measure of PFOT is a highly non-linear function of the weighting factors q_1, q_2, and q_3. If the 'manual' trial and error approach is used to find the desired weighting factor vector, it is a tedious and time-consuming process. Moreover, this approach is not reliable. This is also true for the case of RWA control mode, as shown in Figs. 4.5(d), 4.5(e) and 4.5(f). Using the optimization method, the 'optimal' weighting factor vector for both control modes can be automatically identified. The resulting weighting factor

vectors together with the corresponding control gain matrices are offered in Table 4.1. With the given controller parameters and nominal vehicle system parameters, the performance measures, RWA ratio (ρ_{rwa}) and PFOT (ρ_{off} in meter), can be determined. These performance measures are also provided in Table 4.1.

The weighting factor vectors listed in Table 4.1 and the relationships of RWA ratio and PFOT value versus the corresponding weighting factors shown Fig. 4.5 reveal that the RWA and PFOT control modes have different or conflicting requirements on the weighting factors. For example, as shown in Table 4.1, for the RWA control mode, weighting factor q_1 takes a large value of $10^{9.9419}$, while for the PFOT control mode, weighting factor q_1 takes a relative small value of $10^{-1.5108}$. Thus, the two control modes have conflicting requirement on weighting factor q_1. As shown in Table 4.1, for the PFOT control mode, the low-speed PFOT is 0.8497 m, reducing by 21.87% with respect to the baseline case, while the high-speed RWA ratio takes the value of 0.9782, decreasing by 18.6% compared with that of the baseline case. For the RWA control mode, RWA ratio takes the value of 0.8296, decreasing by 31.0% compared with that of the baseline case, while the low-speed PFOT is 2.2026 m, increasing by 102.53% with respect to the baseline case. The numerical simulation results further demonstrate the well-known fact that for articulated heavy vehicles, the low-speed path-following and

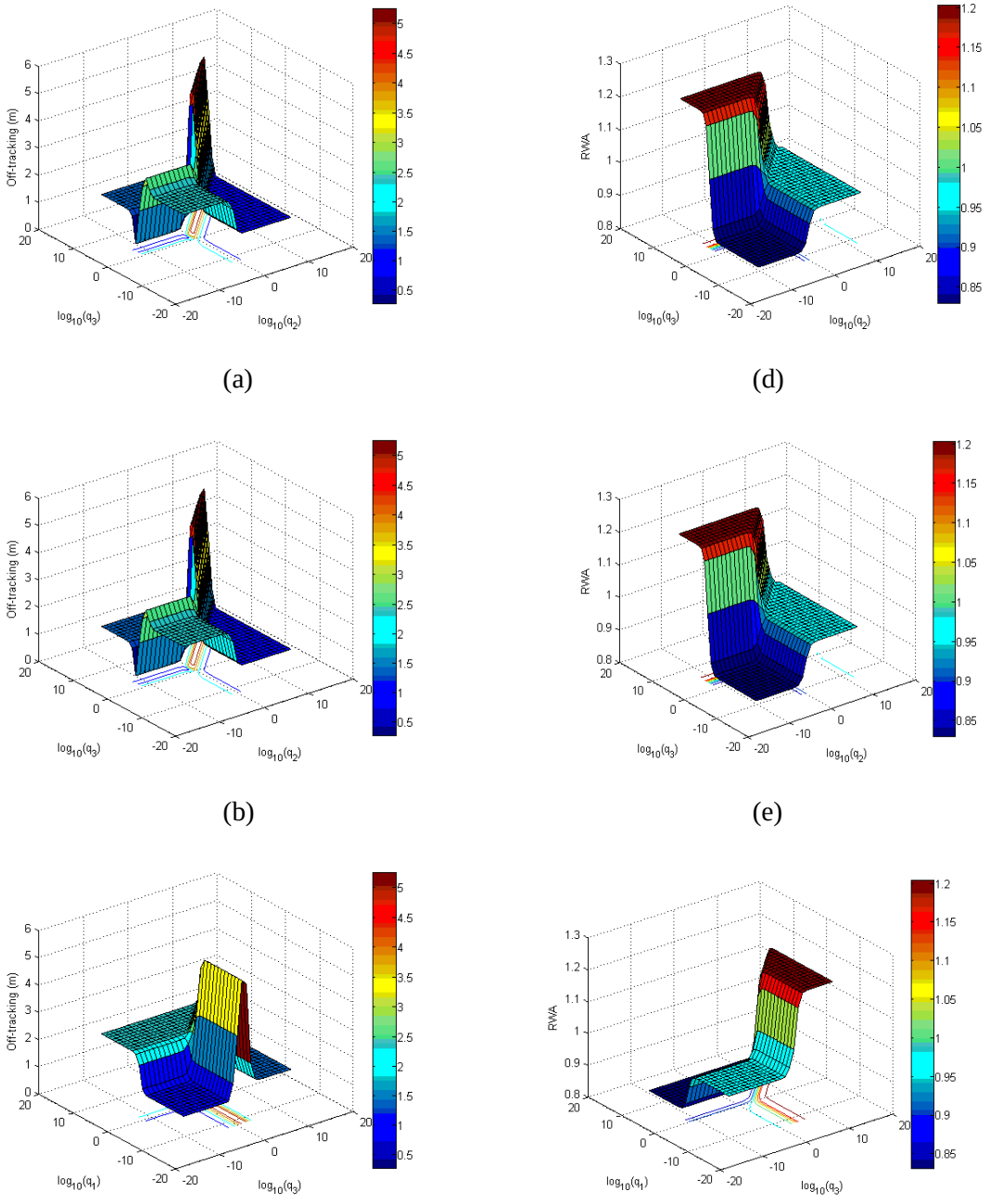

(a) (d)

(b) (e)

(c) (f)

Fig. 4.5: PFOT versus controller weighting factors (low-speed PFOT control mode): (a) PFOT versus q_1 and q_2, (b) PFOT versus q_2 and q_3, and (c) PFOT versus q_1 and q_3; RWA ratio versus weighting factors (high-speed RWA control mode): (d) RWA ratio versus q_1 and q_2, (e) RWA ratio versus q_2 and q_3, and (f) RWA ratio versus q_1 and q_3

high-speed lateral stability have conflicting requirements on design variables [1], active steering tactics that improve high-speed yaw stability (representing by the RWA ratio) typically degrade low-speed path-following when applied at low speeds [28]. Numerical simulations in the current research also identify the interesting phenomenon reported by Wu and Lin [33]: in the high-speed lane change maneuver, with the same steer input used in the baseline case, the vehicle with the RWA control mode can't achieve the required lateral displacement. Comparing Fig. 4.3(b) with Fig. 4.6(a) shows that the vehicle with the RWA control mode will be displaced in lateral direction by 0.465 m instead of 3.7 m in the baseline case. Figs. 4.3(a) and 4.6(b) also indicate that compared with the baseline case, the lateral acceleration level of both the tractor and trailer in the control case is reduced. Obviously, the reduction of the lateral acceleration level leads to the lateral displacement decrease of the tractor and trailer. The reason for reducing the lateral acceleration level can be further tracked by analyzing equation (4.3) and Fig. 4.1. For the RWA control mode, the weighting factor q_1 takes the very large value of $10^{9.9419}$. As indicated in equation (4.3), this large weighting factor imposes penalties upon the magnitude and durations of the lateral acceleration of the tractor, $\dot{V}_1 + U_1\omega_1$. As shown in Fig. 4.7, to achieve the required lane change displacement, the amplitude of the sinusoid steer input should increase from 0.0113 to 0.09.

As expected, with the RWA and PFOT control modes, the tractor/full-trailer system has better low-speed path-following performance and improved lateral stability at high speeds. In the case that the high-speed RWA control system is equipped, the low-speed

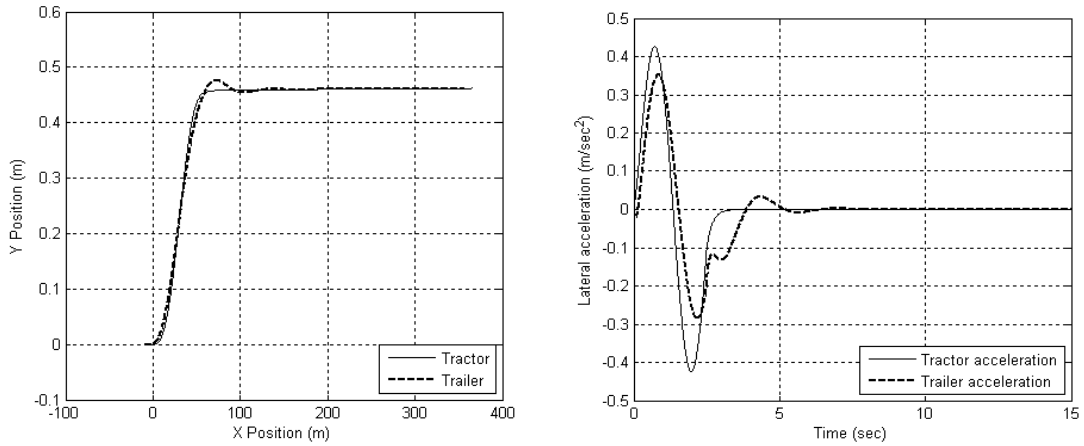

(a) (b)

Fig. 4.6: Control case with RWA control mode in high-speed lane change maneuver (the amplitude of the sinusoid steering input, A, taking the value of 0.0113): (a) trajectory of tractor front axle centre and that of trailer rear axle centre; (b) lateral acceleration at CG of tractor and trailer versus time

PFOT control mode may share the same hardware, e.g. actuators, since these two control modes have the same requirements on the control system configuration. Thus, the introduction of the low-speed control mode may replace the conventional passive trailer steering systems, such as self-steering and command steer systems, for improving low-speed path-following performance. Moreover, from the vehicle design viewpoint, the concept of low-speed control mode provides an alternative way to predict performance envelopes for articulated vehicle low-speed path-following. However, it should be noted that compared with traditional passive trailer steering systems, the low-speed PFOT control mode has the disadvantage of consuming additional energy.

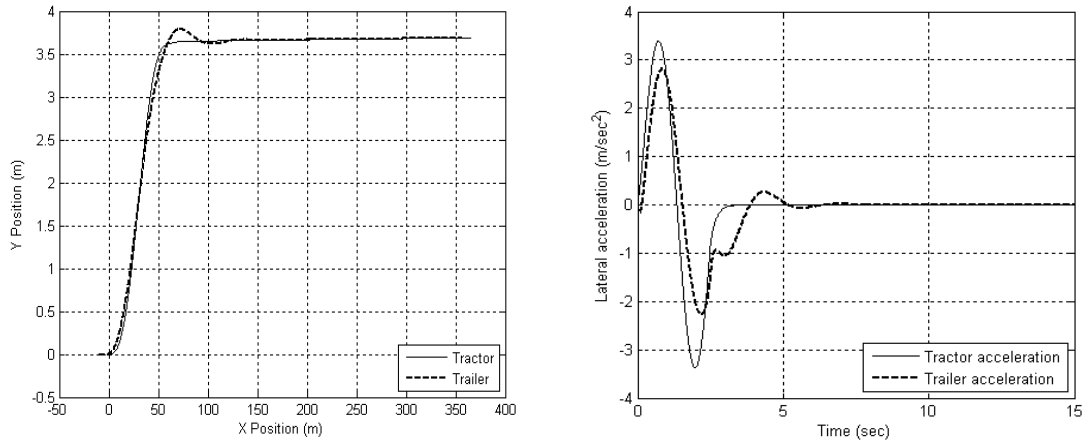

(a) (b)

Fig. 4.7: Control case with RWA control mode in high-speed lane change maneuver (the amplitude of the sinusoid steer input, A, taking the value of 0.09): (a) trajectory of tractor front axle centre and that of trailer rear axle centre; (b) lateral acceleration at CG of tractor and trailer versus time

4.5.3 Simulation Results of Optimal Case

With the performance measures, ρ_{rwa} and ρ_{off}, and the LQR control weighting factor vectors, $[q_{RWA1} \quad q_{RWA2} \quad q_{RWA3}]$ and $[q_{OFF1} \quad q_{OFF2} \quad q_{OFF3}]$, provided in Table 4.1, based on the objective function shown in equation (4.4) and the proposed design synthesis approach described in Fig. 4.2, the optimized vehicle design variable vector **X** and LQR control gain matrices **K** can be determined. Note that in the current research, only trailer parameters are optimized and tractor parameters remain unchanged. The design variable vector **X** includes trailer inertial and geometric parameters. The resultant optimized design variables and control gain matrices are listed in Table 4.2. For the purpose of comparison, Table 4.3 summarizes the performance measures for the three cases, i.e. baseline case, control case, and optimal case.

Table 4.2: Optimized design variables and controller gain matrices

Design variables	**Nominal values**	**Upper bounds**	**Lower bounds**	**Optimized variables**
m_2 (kg)	5460	6006	4914	4914.1
I_2 (kg m^2)	12540	13794	11286	12269
S_4 (m)	2.44	2.684	2.196	2.1960
S_5 (m)	1.68	1.848	1.512	1.512
S_6 (m)	1.37	1.507	1.233	1.233
RWA control gain **K**	[0.0995 -1.1379 -0.0334 -0.05156]			[0.0960 -1.0925 -0.0559 -0.5913]
PFOT control gain **K**	[-0.7043 3.6369 -2.5142 -0.5098]			[-0.7582 3.7544 -2.6505 -0.5632]

Fig. 4.9 shows the simulation results of the optimized vehicle under the high-speed lane change maneuver with the amplitude of the sinusoid steering input A taking the value of 0.09. Fig. 4.8(a) illustrates that in the optimal case, the tractor and trailer first reach the lateral displacement of 3.7 m at 2.56 s and 2.9 s, respectively, while in the baseline case shown in Fig. 4.3(a), the tractor and trailer first achieve this lateral displacement at 5.9 s and 6.4 s, correspondingly. Fig. 4.8(b) demonstrates that in the optimal case, the tractor is able to complete the lane change around a longitudinal distance of 65 m, while in the baseline case shown in Fig. 4.3(b), the tractor requires a distance of 110 m. The trailer trajectories shown in Figs. 4.3(b) and 4.8(b) indicate that compared with the baseline case, the trailer of the optimized vehicle experiences a larger overshoot. Thus, compared with the baseline vehicle, the optimized vehicle responds the

driver command faster and completes the lane change with less distance. Note that as in the control case discussed in the section of Simulation Results of Control Case, to make the optimized vehicle to complete the lane change, the amplitude of the sinusoid steer input *A* should take larger value compared with that used for the baseline vehicle.

Table 4.3: Performance measures for the baseline, control and optimal cases

	Baseline case	**Control case**	**Optimal case**	**Improvement***
RWA (high-speed lane change)	1.2024	0.8296	0.8408	30.01%
PFOT (m) (low-speed circle path following)	1.0875	0.8497	0.7051	35.16%
Transient PFOT (m) (high-speed speed lane change)	0.2362	0.2550	0.2500	-5.84%

* The optimized vehicle performance measurement improvement with respect to the baseline vehicle.

As listed in Table 4.3, compared with the baseline vehicle, the optimized vehicle improves its high-speed lateral stability by 30.01%, decreasing the RWA ratio from 1.2024 of the baseline case to 0.8408. This performance measure improvement is mainly due to the effect of the RWA control mode. As indicated in the previous section, the introduction of the high-speed RWA control mode contributes the RWA ratio reduction of the optimized vehicle. Note that the RWA ratio for the optimized vehicle is 1.35% larger than that of the control case. This RWA ratio increase may be explained by the fact

that the design objective of the optimized vehicle is to achieve a compromised solution between the high-speed lateral stability and low-speed path-following. As to be indicated in the following paragraph, the optimized vehicle achieves the superior low-speed path-following performance at the expense of minor degradation of high-speed lateral stability.

Fig. 4.9 illustrates the trajectory of the tractor axle centre and that of the trailer rear axle centre when the optimized vehicle travels in low-speed circle path-following maneuver. As shown in Table 4.3, compared with the baseline vehicle, the optimized vehicle improves the low-speed path-following by 35.16%, reducing the PFOT from 1.2024 m of the baseline vehicle to 0.7051 m. This low-speed path-following performance improvement is due to the combined effect of introducing low-speed PFOT control mode and finding the optimized trailer design variables. As illustrated in Table 4.3, compared with the baseline vehicle, the introduction of the low-speed PFOT control mode alone can improve the low-speed performance by 21.87%. Built upon this, the effect of optimized design variables can further contribute the low-speed performance improvement. As listed in Table 4.2, for the design variables S_4 (distance between the trailer front axle to the articulation hitch), S_5 (distance between the trailer front axle to its CG) and S_6 (distance between the trailer rear axle to its CG), their optimized values take the corresponding lower bound values. The optimized design variables indicate that in order to improve low-speed path-following, the trailer geometric parameters and its tire base in particular should take values as low as possible. This agrees well with the conclusions offered by Fancher and Winkler [1].

Table 4.3 also offers the transient PFOT values for the three cases in the high-speed lane change maneuver. The optimal and control cases have higher levels of transient PFOT

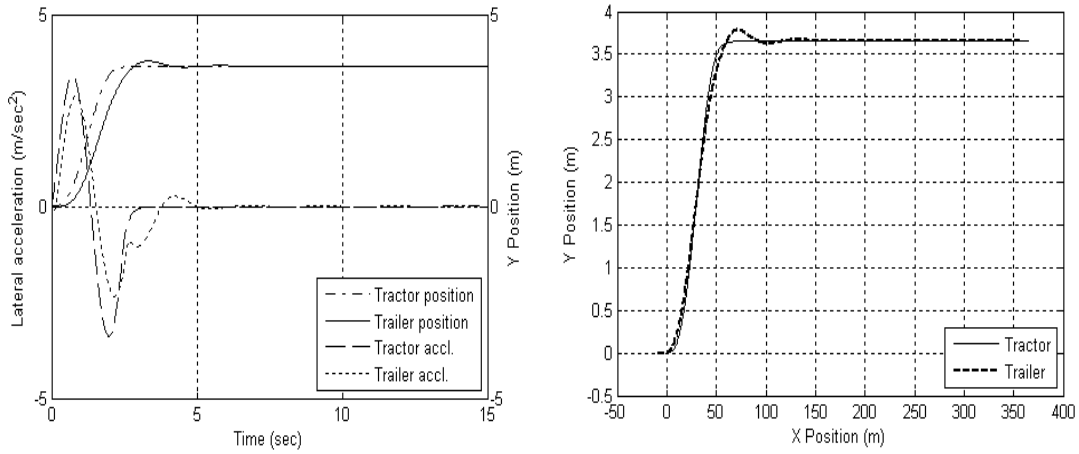

(a) (b)

Fig. 4.8: Optimal case in high-speed lane change maneuver (the amplitude of the sinusoid steer input, *A*, taking the value of 0.09): (a) lateral acceleration at CG of tractor and trailer versus time and lateral displacement of tractor front axle centre and that of trailer rear axle centre versus time; (b) trajectory of tractor front axle centre and that of trailer rear axle centre

than that of the baseline case. A good indication of the relative performance of each case can be observed in the high-speed lane change paths shown in Figs. 4.3(b), 4.7(a) and 4.8(b). The worst performing case is the control case with the RWA control mode. The transient PFOT value in the control case is 8.0% higher than that of the baseline case. Compared with the control case, the optimized vehicle has less transient PFOT value, decreasing from 0.255 m of the control case to 0.25 m. In all cases, the level of transient PFOT is well below the performance measure of 0.8 m proposed by Australia's National Road Transport Commission [32].

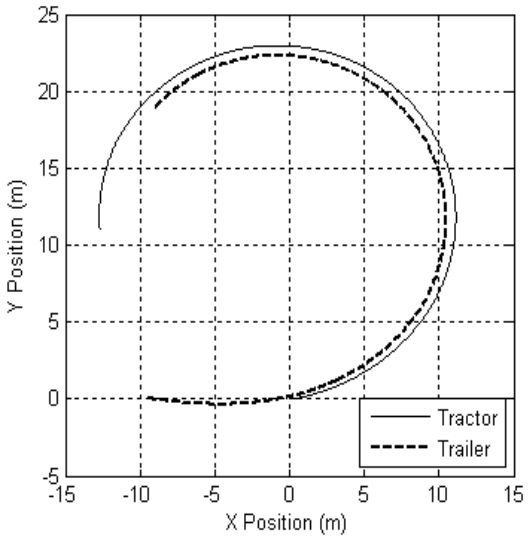

Fig. 4.9: Optimal case in low-speed circle path-following maneuver (with a step steer input of $\delta_{max} = 0.061\pi$): trajectory of tractor front axle centre and that of trailer rear axle centre

Among the three cases listed in Table 4.3, the optimized vehicle has the best overall performance in terms of high-speed lane change RWA ratio, low-speed PFOT value, and high-speed lane change transient PFOT. This superior overall performance of the optimized vehicle is due to the integrated design optimization of the trailer's inertial and geometric parameters as well as the active trailer steering system with the RWA and PFOT control modes.

4.6 CONCLUSIONS

This chapter proposes the two loop design (TLD) method for active trailer steering (ATS) systems of articulated heavy vehicles (AHVs). To improve the overall performance of AHVs, the passive vehicle design variables, such as trailer geometric and inertial parameters, and the active design variables of ATS systems, e.g. the control gain matrices

of the optimal controller based on the linear quadratic regular (LQR) theory, can be optimized simultaneously. In order to coordinate the conflicting performance requirements of the low-speed path-following and the high-speed lateral stability of AHVs, the LQR controller has two operational modes: the low-speed PFOT (Path-Following Off-Tracking) control mode is designed in such a way that in a low-speed circle path-following maneuver, the PFOT of the AHV is minimized; the high-speed RWA control mode is developed following the idea that the vehicle system is optimized to make the Rear-Ward Amplification (RWA) ratio as small as possible in the high-speed single lane change maneuver. In the design of the LQR controller, the weighting factor vectors are determined using an optimization method instead of the conventional trial and error approaches.

To demonstrate the feasibility and effectiveness of the proposed design method, it is applied to the design of a front trailer axle active steering system for a tractor/full-trailer combination based on a 3 degree-of-freedom (DOF) linear yaw plane model. The active steering control strategy is explained from a vehicle dynamic viewpoint. An instrumentation arrangement for implementing this control is recommended. Simulation results illustrate that in comparison to the baseline vehicle, the one derived from the design synthesis approach decreases the low-speed PFOT by 35.16% and reduces the high-speed RWA ratio by 30.01%. The proposed approach may be used for identifying desired design variables and predicting performance envelopes in the early design stages of AHVs with ATS systems.

Chapter 5

SINGLE DESIGN LOOP METHOD FOR THE DESIGN OF AHVS WITH ATS SYSTEMS

5.1 INTRODUCTION

This chapter presents an automated design synthesis approach, called a single loop (SDL) method, for articulated heavy vehicles (AHVs) with active trailer steering (ATS) systems. AHVs have poor maneuverability when traveling at low speeds. Moreover, AHVs exhibit unstable motion modes at high speeds. To address the problem of maneuverability, 'passive' trailer steering systems have been developed. These systems improve low-speed performance, but feature with low lateral stability at high speeds. Some ATS systems have been proposed to improve high-speed lateral stability. However, these systems typically degrade maneuverability when applied at low speeds. To tackle this conflicting design problem, a systematic method is proposed for the design of AHVs with ATS systems. This new design method has the following features: the optimal active design variables of the ATS systems and the optimal passive design variables of the vehicle are identified in a single design loop; in the design process, to evaluate the vehicle performance measures, a driver model is introduced and it 'drives' the vehicle model based on the well-defined testing specifications. Through the design optimization of an ATS system for an AHV with a tractor and a full trailer, this SDL method is compared

against the two design loop (TDL) method, presented in the previous chapter. The benchmark investigation shows that the former can determine better trade-off design solutions than those derived by the latter. This SDL method provides an effective approach to automatically implement the design synthesis of AHVs with ATS systems.

The rest of this chapter is organized as follows. Section 5.2 introduces the driver model and the test maneuver emulated for evaluating the AHV performance at low and high speeds. Moreover, the construction of the LQR controller for ATS systems is outlined in the same section. The proposed SDL method is presented in Section 5.3. Section 5.4 compares the design results derived from the SDL approach against those based on the TDL method. Finally, conclusions are drawn in Section 5.5.

5.2 VEHICLE SYSTEM MODELS

5.2.1 Vehicle Model

The proposed SDL method is examined and evaluated by applying it in design of a tractor/full-trailer system as used in the previous chapter. The details of the vehicle model (called as Model-1), utilized in this chapter to determine the directional performance measure of the vehicle system, is described in Subsection 3.2.1.

5.2.2 Maneuvers emulated

Two test maneuvers, i.e. the 90-degree intersection turn [32] and the single-lane change specified in SAE J2179 [35], are widely accepted for measuring low-speed PFOT and

high-speed RWA ratio of AHVs, respectively. In each of the maneuvers, the vehicle tested is required to follow a precisely prescribed path at a specified speed and the diver should continuously monitor and adjust steering actions accordingly. In the current research, the recommended single lane change test procedure has been simulated for determining the high-speed RWA ratio. In this simulation, the vehicle is traveling at the speed of 88 km/h along a straight path section. Then, a sudden lane change is conducted. The lateral displacement of the vehicle in the lane change is 1.46 m. The maneuver emulated during the design process for measuring low-speed PFOT is based on the 90-degree intersection turn test procedure. In this case, the center of tractor front axle is required to travel along a specified path. The vehicle travels at the constant speed of 4 km/h. Moreover, to compare the low-speed PFOT of the optimal designs against that of baseline vehicles, the test maneuver similar to the 360-degree roundabout defined in the United Kingdom's Road Vehicles Regulation [32] has also emulated in the research.

5.2.3 Driver Model

The driver model developed in the research is based on a modified PID control technique. The driver model is to 'drive' the vehicle along the prescribed path. The vehicle steering angle correction is made through the PID control of the vehicle position error. The position error is defined as the distance from the tractor's front axle center to the desired point on the specified path measured along the corresponding radius of curvature.

As shown in Fig. 5.1, the prescribed path is defined by a series of point, (X_i, Y_i), $i = 1,2,.,m$, in the global coordinate system $X - Y$. The position vectors of the tractor

CG, tractor front axle center and the target point on the path are denoted as **r**, $\mathbf{r_f}$, and $\mathbf{r_d}$, respectively. In the global coordinate system, these vectors are expressed as

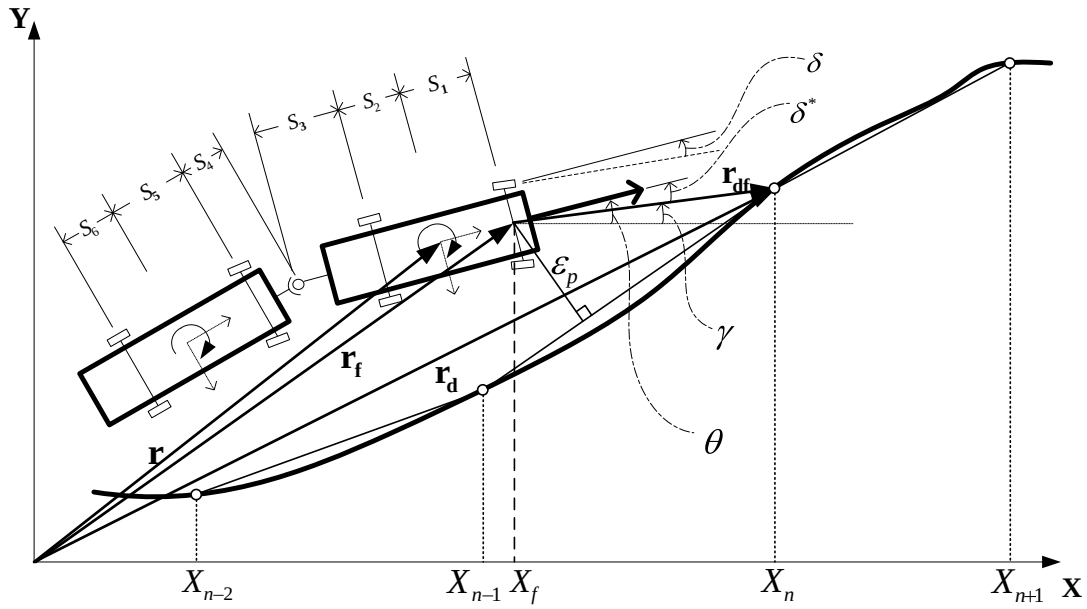

Fig. 5.1: Geometry representation of vehicle and prescribed path

$$\mathbf{r} = X\,\mathbf{i} + Y\,\mathbf{j} \tag{5.1a}$$

$$\mathbf{r_f} = X_f\,\mathbf{i} + Y_f\,\mathbf{j} \tag{5.1b}$$

$$\mathbf{r_d} = X_d\,\mathbf{i} + Y_d\,\mathbf{j} \tag{5.1c}$$

where **i** and **j** are unit vectors in X and Y directions, respectively. If the initial position of tractor CG and the angle swept from the longitudinal axis of the tractor to the X-axis are (X_0, Y_0) and θ_0, respectively, the corresponding position of the tractor front axle center (X_{f_0}, Y_{f_0}) can be determined as

$$X_{f_0} = X_0 + S_1 \cos\theta_0 \tag{5.2a}$$

$$Y_{f_0} = Y_0 + S_1 \sin\theta_0 \tag{5.2b}$$

In the simulation of the high speed single lane change test maneuver, at an arbitrary time instant t, the vehicle position error, $\varepsilon_p(t)$, is defined as follows. Assume that at this instant, the position of the tractor front axle center is $(X_f(t), Y_f(t))$, and on the prescribed path the two adjoining points close to the tractor front axle center are (X_{n-1}, Y_{n-1}) and (X_n, Y_n). If $X_{n-1} < X_f(t) \leq X_n$, point (X_n, Y_n) is selected as the target point on the prescribed path. The vehicle position error $\varepsilon_p(t)$ is defined as the distance measured from the point $(X_f(t), Y_f(t))$ to the straight line connecting the points (X_{n-1}, Y_{n-1}) and (X_n, Y_n). In the simulations of the 90-degree intersection turn and 360-degree roundabout test maneuvers, the vehicle position error $\varepsilon_p(t)$ is defined as the distance between the point $(X_f(t), Y_f(t))$ and the corresponding point on the prescribed path measured along the radius of curvature.

The desired vehicle heading direction can be represented with the position vector defined by

$$\mathbf{r_{df}}(\mathrm{t}) = \mathbf{r_d}(\mathrm{t}) - \mathbf{r_f}(\mathrm{t}) \tag{5.3}$$

The angle swept from vector $\mathbf{r_{df}}(\mathrm{t})$ to $X-$axis is denoted as $\gamma(\mathrm{t})$. The pseudo vehicle steering angle $\delta^*(\mathrm{t})$ can be determined by

$$\delta^*(\mathrm{t}) = \theta(\mathrm{t}) - \gamma(\mathrm{t}) \tag{5.4}$$

where $\theta(\mathrm{t})$ is the angle swept from the longitudinal axis of the tractor to the X-axis at the time instant t. The vehicle steering angle correction $\delta(\mathrm{t})$ at this instant is defined as

$$\delta(\mathrm{t}) = \delta^*(\mathrm{t})p(\mathrm{t}) \tag{5.5}$$

where $p(t)$ is a control variable determined using the following PID control of the vehicle position error.

$$p(t) = K_p\varepsilon_p(t) + K_i\int_0^t \varepsilon_p(\tau)d\tau + K_d\frac{d}{dt}\varepsilon_p(t) \tag{5.6}$$

In equation (5.6), K_p, K_i and K_d represent the proportional, integral and derivative controller gains, respectively.

With the vehicle steering angle input $\delta(t)$, the differential equation of the vehicle model, as shown in equation (3.3), can be solved in the time interval from t to $t + \Delta t$. Tractor lateral velocity $V_1(t + \Delta t)$ and yaw rate $\omega_1(t + \Delta t)$ can be determined. If the time increment Δt is very small, the vehicle heading angel increment $\Delta\theta(t)$ can be calculated by

$$\Delta\theta(t) = -\frac{\omega_1(t)+\omega_1(t+\Delta t)}{2}\Delta t \tag{5.7}$$

Note that the direction of yaw rate ω_1 and that of vehicle heading angle θ are opposite. Thus, the resulting heading angle at the time instant $t + \Delta t$ is

$$\theta(t + \Delta t) = \theta(t) + \Delta\theta(t) \tag{5.8}$$

Over the time interval Δt, the position variation of the tractor CG can be determined using the constant vehicle forward speed U_1 and the instantaneous vehicle lateral speed $V_1(t+\Delta t)$.

$$\Delta X(t) = U_1 \cos\left(\frac{\theta(t)+\theta(t+\Delta t)}{2}\right)\Delta t + \frac{V_1(t)+V_1(t+\Delta t)}{2}\sin\left(\frac{\theta(t)+\theta(t+\Delta t)}{2}\right)\Delta t \tag{5.9a}$$

$$\Delta Y(t) = U_1 \sin\left(\frac{\theta(t)+\theta(t+\Delta t)}{2}\right)\Delta t - \frac{V_1(t)+V_1(t+\Delta t)}{2}\cos\left(\frac{\theta(t)+\theta(t+\Delta t)}{2}\right)\Delta t \tag{5.9b}$$

Then at the time instant $t+\Delta t$, the position of tractor CG and its front axle center can be determined by

$$X(t+\Delta t) = X(t) + \Delta X(t) \tag{5.10a}$$

$$Y(t+\Delta t) = Y(t) + \Delta Y(t) \tag{5.10b}$$

and

$$X_f(t+\Delta t) = X(t+\Delta t) + S_1\cos\left(\theta(t+\Delta t)\right) \tag{5.11a}$$

$$Y_f(t+\Delta t) = Y(t+\Delta t) + S_1\sin\left(\theta(t+\Delta t)\right) \tag{5.11b}$$

respectively. Following the same procedure described above, the vehicle steering angle input $\delta(\mathrm{t}+\Delta t)$ at the time instant $t+\Delta t$ can be determined.

To validate the developed driver model, it has been integrated with the 3-DOF vehicle model and the numerical simulations for the low-speed 90-degree intersection turn and high-speed single lane change test maneuvers have been conducted. Note that in these simulations, the vehicle system parameters take their nominal values provided in Table B1 of Appendix B. Fig. 5.2 shows the simulated trajectory of the tractor front axle center

and the prescribed path for the high-speed test maneuver specified in SAE J2179 [11]. Fig. 5.3 illustrates the fidelity of the simulated trajectory of the tractor front axle center tracking the prescribed path in the 90-degree intersection turn maneuver. The simulation results from both the high and low speed test maneuvers indicates that the vehicle model is well-controlled by the driver model and accurately follows the desired paths.

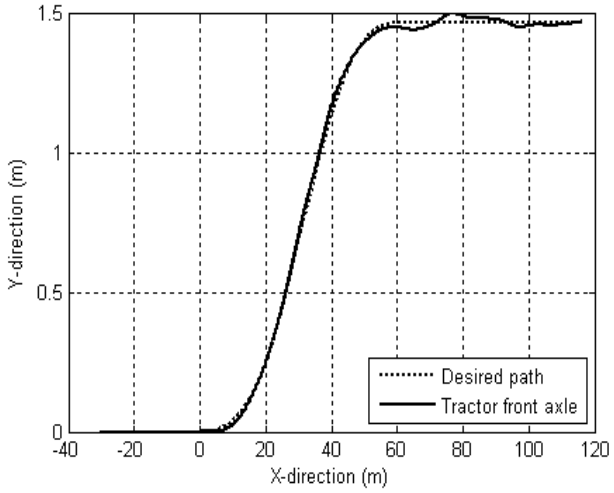

Fig. 5.2: Simulated trajectory of the tractor front axle center from the high-speed single lane change maneuver

5.2.4 LQR Controller for ATS Systems

As shown in Fig. 1, the front axle of the full trailer is steerable and the steering angle δ_r is determined by the optimal controller based on the linear quadratic regular (LQR) theory [37].

The design criterion of the controller is to minimize the tractor/full-trailer system's RWA ratio at high speeds and PFOT value at low speeds. The LQR controller design is

an optimization problem: minimize the performance index, as shown in equation (3.19) subject to equation (3.3). By solving the algebraic Ricatti equation, the solution of the optimization problem is the control vector of the form equation (3.20), where **K** is the control gain matrix with a dimension of 1×4, **x** and **u** are the state and control variable vectors defined by equations (3.4) and (3.5), respectively. In equation (4.1), q_1, q_2 and q_3 are the weighting factors that impose penalties upon the magnitude and duration of the lateral acceleration of the tractor CG, $\dot{V}_1 + U_1\omega_1$, the lateral acceleration of the trailer CG, $\dot{V}_2 + U_2\omega_2$, and the active steering angle, δ_r, respectively. Note that the third term on the right side of equation (4.1) represents the energy consumption of the active trailer steering system.

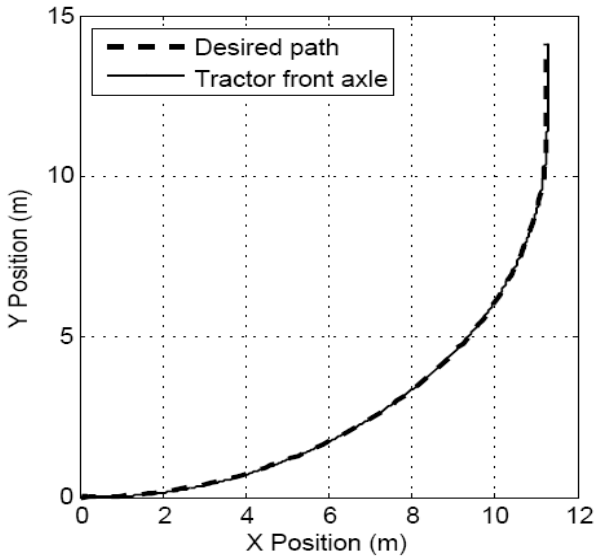

Fig. 5.3: Simulated trajectory of the tractor front axle center from the low-speed 90-degree intersection turn maneuver

In the current research, the LQR controller designed for the ATS systems has two operational modes, one for improving lateral stability at high speeds and the other for

enhancing path-following at low speeds. Based on equation (4.1), for these two control modes, the weighting factor vectors are denoted as $[q_{RWA1} \quad q_{RWA2} \quad q_{RWA3}]$ and $[q_{PFOT1} \quad q_{PFOT2} \quad q_{PFOT3}]$, respectively. Accordingly, the control gain vectors based on equation (3.5) are represented as $\mathbf{K}_{RWA}$ and $\mathbf{K}_{PFOT}$.

5.3 AUTOMATED DESIGN SYNTHESIS APPROACH

Fig. 5.5 shows the preliminary framework of the proposed automated design synthesis approach for AHVs with ATS systems. The design optimization of AHVs is implemented using a genetic algorithm (GA). The AHV model may be generated using multibody dynamic programs, e.g. ADAMS and TruckSim. The ATS controller based on LQR technique and the driver model can be constructed in Matlab. Then, the combined vehicle model, ATS controller and driver model are optimized simultaneously using the GA.

As shown in Fig. 5.5, a population of n sets of design variables evaluated by the GA is sent forward in parallel to the AHV model, ATS controller and driver model. For a given design variable set $\mathbf{X}$, it includes $\mathbf{X}_{SYS}$, $\mathbf{X}_{RWA}$ and $\mathbf{X}_{PFOT}$. Note that in the current research $\mathbf{X}_{SYS}$ represents passive vehicle system parameters, such as the trailer geometric and inertia parameters, $\mathbf{X}_{RWA}$ denotes $[q_{RWA1} \quad q_{RWA2} \quad q_{RWA3}]$, and $\mathbf{X}_{PFOT}$ stands for $[q_{PFOT1} \quad q_{PFOT2} \quad q_{PFOT3}]$. With this set of design variables, the vehicle system model is generated, and the LQR controller and driver model are constructed. Then, the driver model will ‘drive’ the vehicle model in both the high-speed single lane change maneuver and the low-speed 90-degree interaction turn maneuver, respectively. In these two

maneuvers, the LQR controller operates in its high-speed RWA and low-speed PFOT control modes, accordingly. The corresponding data processor determines the resulting performance measure, RWA representing $F_{RWA}(\mathbf{X}_{SYS}, \mathbf{X}_{RWA})$ and PFOT denoting $F_{PFOT}(\mathbf{X}_{SYS}, \mathbf{X}_{PFOT})$. These performance measures are to be used for the cost function evaluation in the form of the following utility function.

$$obj = \frac{\sigma_1}{\rho_{RWA}} \cdot F_{RWA}(\mathbf{X}_{SYS}, \mathbf{X}_{RWA}) + \frac{\sigma_2}{\rho_{PFOT}} \cdot F_{PFOT}(\mathbf{X}_{SYS}, \mathbf{X}_{PFOT}) \tag{5.12}$$

where ρ_{RWA} and ρ_{PFOT} denotes RWA ratio and PFOT value of the baseline vehicle for high speed lane change and low speed turning maneuvers, respectively, σ_1 and σ_2 are two constants. Corresponding to the n sets of design variables, the resulting fitness value vector $[obj_1 \quad obj_2 \quad ... \quad obj_n]$ can be achieved. At this point, if the convergence criteria are satisfied, the calculation terminates; otherwise, this vector is sent back to the GA. Based on the returned fitness values corresponding to the given sets of design variables, the GA produces the next generation of design variable sets using selection, crossover, and mutation operators. This procedure repeats until the optimized variable set is found.

With the above automated design synthesis approach, all optimal design variables, including the weighting factors for constructing the LQR controller, LQR controller gains, and passive vehicle system design variables, can be identified in a single design loop (SDL). Compared with the two design loop (TDL) method recommended in Ref.

[12], the proposed SDL approach is more suitable for automated design process of AHVs.

5.4 RESULTS AND DISCUSSION

In this section, the simulation results from the SDL method are discussed and compared with those from the TDL approach reported in Ref. [12]. To make the results from the two design methods comparable, in both cases, the driver model has been incorporated in the simulated test maneuvers. Both design methods have been applied to the design synthesis of an AHV with ATS systems using the 3-DOF vehicle model. The baseline vehicle system parameters are provided in Table B1 of Appendix B. In the case of TDL method, in the first design loop, the design variables are the weighting factor vectors $[q_{RWA1} \quad q_{RWA2} \quad q_{RWA3}]$ and $[q_{PFOT1} \quad q_{PFOT2} \quad q_{PFOT3}]$, which are used to constructed the LQR controllers for the RWA and PFOT control modes. In the second design loop, the design variables consists of the trailer geometric and inertia parameters, including m_2, I_2, S_4, S_5 and S_6, and controller gain vectors $\mathbf{K}_{RWA}$ and $\boldsymbol{K}_{PFOT}$ for the RWA and PFOT control modes, respectively. In the case of SDL method, the optimized values of all the above design variables are found in a single design loop.

With an operation of the SDL method shown in Fig. 5.4, the optimized values of the design variables have been found and they are listed in Table 5.1 together with the nominal values of the passive design variables.

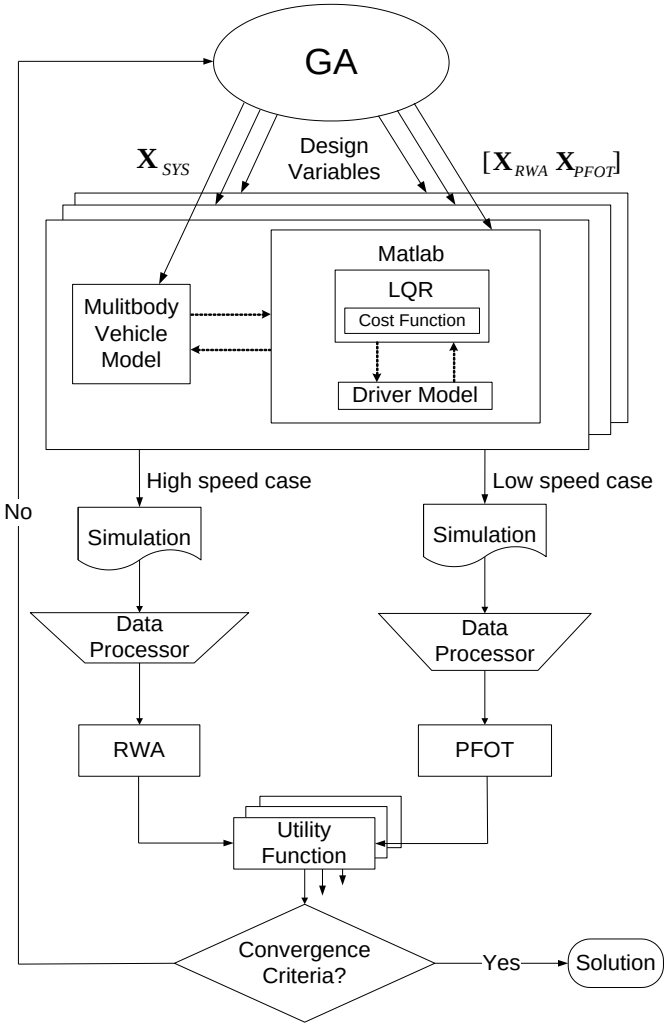

Fig. 5.4: Schematic representation of the automated design synthesis approach

In the SDL and baseline design cases, the selected resulting vehicle dynamic responses are illustrated in Figs. 5.5, 5.6, 5.7 and 5.8. Note that in the baseline vehicle case, the vehicle system parameters take their nominal values offered in Appendix B and the trailer is non-steerable. Fig. 5.5 shows the time history of the lateral accelerations of the tractor and trailer CG in the high speed single lane change maneuver for both the

baseline and SDL designs. Due to the RWA control mode of the ATS system and the optimal passive design variables derived from the SDL method, the RWA ratio decreases by 48.67%, changing from the baseline value of 1.573 to 0.8074. The drop of the RWA ratio will greatly improve the high-speed lateral stability to the resulting design.

Fig. 5.6 provides useful simulation results for investigating whether the trailer can follow the tractor's trajectory accurately in the high-speed lane change maneuver. Compared with the baseline vehicle, in the case of the SDL design, the trailer follows the tractor's path more accurately with the maximum transient PFOT of 0.3048 m, decreasing 5.78% from the corresponding baseline value of 0.3235 m. Results shown in Figs 5.5 and 5.6 imply that with respect to the baseline design, in the case of the SDL design, the vehicle system has higher lateral stability and the trailer can more accurately follow the tractor's path in high-speed obstacle avoidance situations.

With the simulation results shown in Fig. 5.7, the SDL design's low-speed maneuverability can be examined and evaluated. Fig. 5.7(a) offers the simulation result of the baseline design, illustrating the trajectory of the tractor's front axle center and that of the trailer's rear axle center in the low-speed 90-degree intersection turn test maneuver. Fig. 5.7(b) shows the corresponding simulation result for the SDL design. A close observation of the simulation results reveals that compared with the baseline design, in the case of the SDL design, the trailer can track the tractor trajectory more closely. For the SDL design, the maximum PFOT (Path-Following Off-Tracking) value

drops by 29.74%, decreasing from the baseline value of 1.2818 m to the SDL value of 0.9006 m. Simulation results shown in Fig. 5.8 further demonstrate the low-speed performance improvement of the SDL design compared against the baseline vehicle. In

Table 5.1: Optimized values for passive and active design variables derived from one operation of the SDL method

Design variables	**Nominal values**	**Lower bounds**	**Upper bounds**	**Optimized variables**
m_2 (kg)	5460	5187	5733	5675.6
I_2 (kg m^2)	12540	11913	13167	12255
S_4 (m)	2.44	2.318	2.562	2.3366
S_5 (m)	1.68	1.596	1.764	1.6039
S_6 (m)	1.37	1.3015	1.4385	1.3506
$\log_{10}(q_{RWA1})$		-10	10	3.4747
$\log_{10}(q_{RWA2})$		-10	10	-1.4240
$\log_{10}(q_{RWA3})$		-10	10	4.7494
$\log_{10}(q_{PFOT1})$		-10	10	0.7329
$\log_{10}(q_{PFOT2})$		-10	10	0.3307
$\log_{10}(q_{PFOT3})$		-10	10	0.8975
Controller gain $\mathbf{K}_{RWA}$ for RWA mode				[0.0908 -1.0381 -0.0342 -0.4873]
Controller gain $\mathbf{K}_{PFOT}$ for PFOT mode				[-2.5808 7.8148 -5.3475 -1.1963]

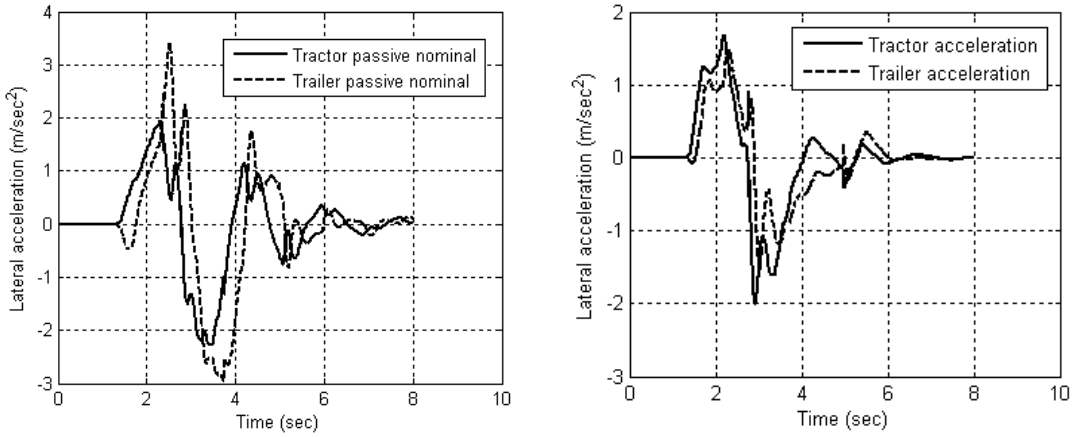

(a) (b)

Fig. 5.5: Lateral acceleration at CG of tractor and trailer versus time (results achieved in the simulated high-speed lane change maneuver): (a) baseline design case; (b) SDL design case

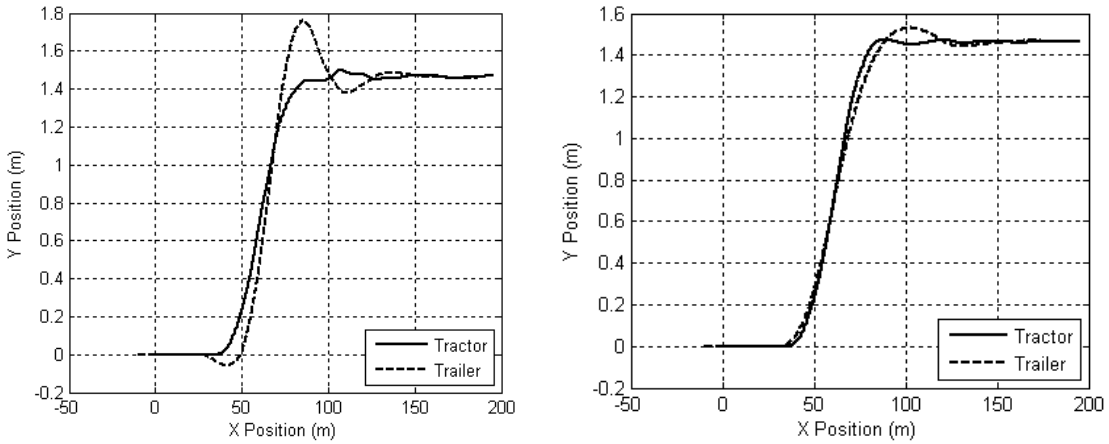

(a) (b)

Fig. 5.6: Trajectory of track front axle center and that of trailer rear axle center (results achieved in the simulated high-speed lane change maneuver): (a) baseline design case; (b) SDL design case

the case of the baseline design, Fig. 5.8(a) offers the simulation result of the trajectory of the tractor's front axle center and that of the trailer's rear axle center in the low-speed 360-degree roundabout test maneuver. Fig. 5.8(b) provides the corresponding result for the SDL design. The simulation results offered in Fig. 5.8 indicate that the steady state PFOT value of the SDL design is 3.56% lower than that of the baseline design,

decreasing from the baseline value of 1.0872 m to 1.0485 m. The low-speed performance improvement of the SDL design is attributed to the PFOT control mode of the ATS system and the optimal passive design variables derived from this design method.

To summarize the performance measures for both of the baseline and SDL designs, Table 5.2 lists the quantitative simulation results. As shown in this table, compared with the baseline vehicle, the SDL design has better performance in all the four aspects, i.e. RWA ratio, PFOT value in both of the two simulated low-speed test maneuvers, and the transient PFOT in the high-speed lane change test procedure.

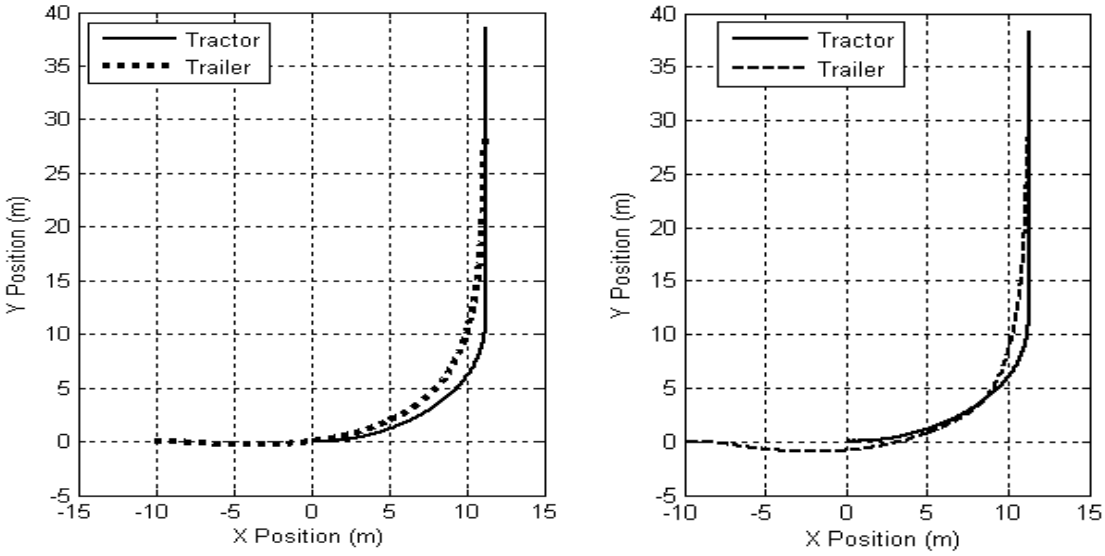

(a) (b)

Fig. 5.7: Trajectory of tractor's front axle center and that of trailer's rear axle center (results achieved in the simulated low-speed 90-degree intersection turn maneuver): (a) baseline design case; (b) SDL design case

Table 5.2 also provides the simulation results of the TDL design. Note that in the cases of SDL and TDL, the optimal results shown in this table have been derived from the

corresponding design approaches and a single run of the GA (genetic algorithm). In the implementation of the global search algorithm, the feasible variation ranges of the passive design variables for the two methods are the same as listed in Table 5.1. In the design optimizations using the GA, the population size and total number of generations took the values of 80 and 200, respectively.

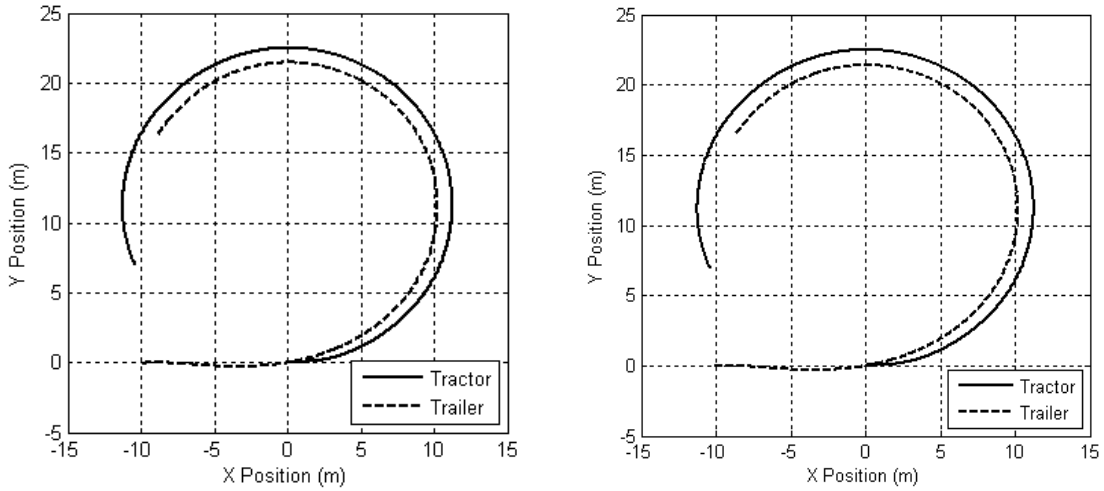

Fig. 5.8: Trajectory of tractor's front axle center and that of trailer's rear axle center (results achieved in the simulated low-speed 360-degree roundabout maneuver): (a) baseline design case; (b) SDL design case

Compared with the TDL design, the vehicle based on the SDL method has better low-speed performance, lowering the 90-degree turn PFOT value by 2.0% from the TDL value of 0,9189 m. In terms of the 360-degree roundabout PFOT value, RWA ratio and transient PFOT under high-speed lane change, these two designs are very close. Base on the results offered in Table 5.2, it seems that there is no big difference between the two designs in terms of the low and high speed performance. However, in multi-objective

design optimization problems, such as the one discussed in this paper, considerable emphasis is often placed on the trade-off analysis for a bunch of solutions instead of focusing on a single design.

Table 5.2: Performance measures for the baseline vehicle, SDL and TDL designs

Performance measures	**Baseline case**	**TDL case**	**SDL case**	**Improvement***
RWA ratio (high-speed lane change)	1.5730	0.8072	0.8074	48.67
PFOT value/m (low-speed 90-degree intersection turn)	1.2818	0.9189	0.9006	29.74
PFOT value/m (low-speed 360-degree roundabout)	1.0872	1.0497	1.0485	3.56
Transient PFOT/m (high-speed speed lane change)	0.3235	0.3048	0.3048	5.78

* Improvement of the SDL case compared against the baseline vehicle.

Fig. 5.9(a) illustrates all the design solutions derived from the SDL method in terms of the relationship between the RWA ratio and PFOT value in the 90-degree intersection turn maneuver. Note that the results provided are achieved from several operations of the SDL method with different value combinations of the weight factors σ_1 and σ_2 shown in equation (5.12). Similarly, Fig. 5.9(b) shows the design solutions obtained from the TDL method. In Fig. 5.9, the individual designs from the GA are represented by circles, which tend to cluster as the GA converges to the optimal designs. The comparison of the results shown in Fig. 5.9(a) and those in Fig. 5.9(b) indicates that the circles representing the

design solutions from the TDL method are situated in a limited area, but those from the SDL method are scattered in a much larger area. This phenomenon can be explained by the different features of the TDL and SDL design methods. As introduced previously, the TDL method searches optimal designs through two design loop. In the first design loop, the passive vehicle parameters take their nominal values and a set weighting factors for the LQR controller including $[q_{RWA1}\ q_{RWA2}\ q_{RWA3}]$ and $[q_{PFOT1}\ q_{PFOT2}\ q_{PFOT3}]$ are determined. Then, in the second design loop, with the given set LQR controller weighting factors, the passive vehicle design variables are determined. However, the SDL method treats the entire LQR controller weighting factors and passive vehicle parameters as the design variables and searches the optimal designs in a single design loop. Therefore, the design variable space for the SDL method is much larger than that of the TDL method. Consequently, the design solution space from the SDL method is larger than that from the TDL method. Since the TDL design method limits its design variable space, it may exclude some good design solutions.

A close observation of Fig. 5.9(a) reveals that the densely-clustered optimal designs can be classified into three sets, namely, RWA set, Pareto set and PFOT set. These three optimal design solution sets are dependent on the values of the design variables $[q_{RWA1}\ \ q_{RWA2}\ \ q_{RWA3}]$, $[q_{PFOT1}\ \ q_{PFOT2}\ \ q_{PFOT3}]$ and the values the weight factors σ_1 and σ_2. For example, if σ_2 takes the value of zero, the multi-objective design optimization problem shown in equation (5.14) reduces to a mono-objective design

optimization problem. This will result in the RWA optimal design set. Thus, the performance measures of the RWA ratio and the PFOT value are independent each other.

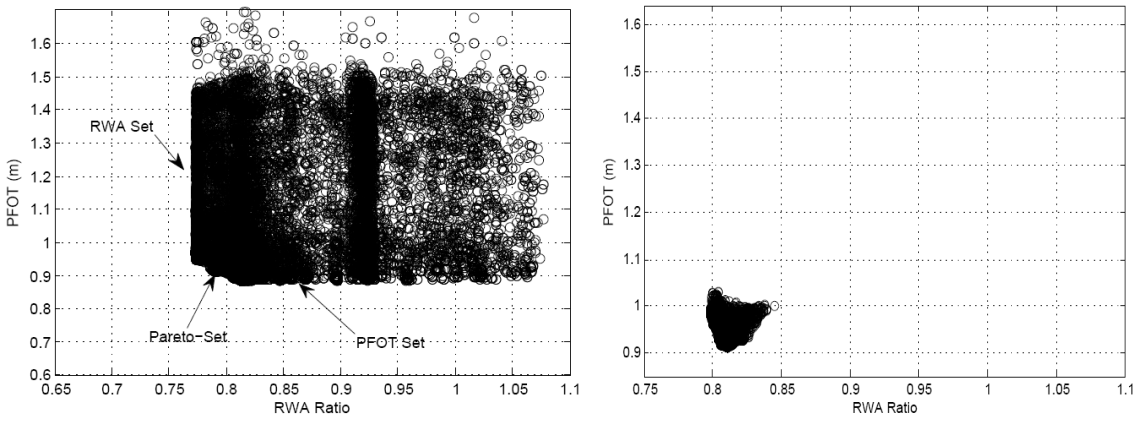

Fig. 5.9: Relationship between RWA ratio and PFOT: (a) SDL design case; (b) TDL design case

Similarly, if σ_1 takes the value of zero, this will lead to the PFOT optimal design set. Moreover, if none of σ_1 and σ_2 takes zero value and the both $[q_{RWA1} \quad q_{RWA2} \quad q_{RWA3}]$, and $[q_{PFOT1} \quad q_{PFOT2} \quad q_{PFOT3}]$ are not a null vector, the Pareto optimal design set can be achieved. Results shown in Fig. 5.9 indicate that compared with the TDL approach, the SDL method can provide a much more comprehensive design solution set.

Fig. 5.10 provides the Pareto optimal design solution sets derived from the SDL and TDL design methods. Note that the results shown in Fig. 5.10 are based on the curve fitness from the results offered in Fig. 5.9. As shown in Fig. 5.10, the SDL method provides better trade-off design solutions than the TDL method.

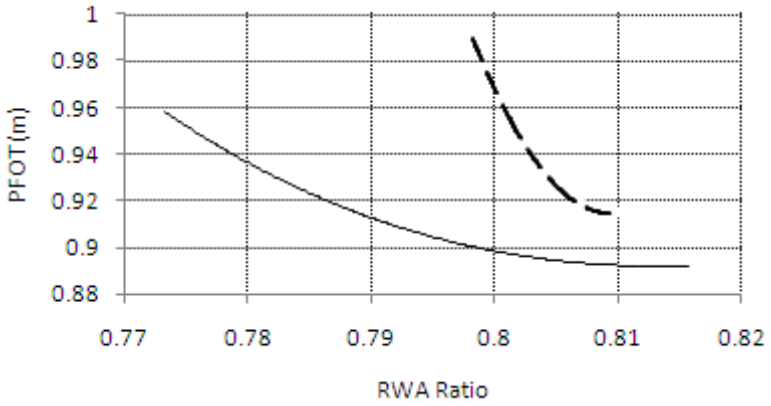

Fig. 5.10: Trade-off design solutions derived from SDL method (solid line) and TDL method (dashed line)

5.5 CONCLUSIONS

This chapter presents an automated design synthesis approach, called Single Design Loop (SDL) method, for the design of articulated heavy vehicles (AHVs) with active trailer steering (ATS) systems. The proposed design method has the following distinguished features: 1) the optimal active design variables of the ATS systems and the optimal passive vehicle system design variables are searched in a single design loop; 2) in the design process, to evaluate the vehicle performance measures, a driver model is introduced and it 'drives' the vehicle model based on the well-defined testing specifications. The ATS systems derived from this design method have two operational modes, one for improving the lateral stability at high speeds and the other for enhancing the path-following at low speeds. With the suggested combination of multibody vehicle

modeling/simulation technique and optimization algorithms, the SDL method is suitable for the automated design synthesis of AHVs with ATS systems.

The proposed SDL method has been applied to the design of an AHVs with ATS systems using a 3 degrees of freedom vehicle model. An optimal design derived from this method is compared with the baseline vehicle. Numerical simulation results show that the optimal design is superior to the baseline vehicle in the performance measures of high-speed lateral stability and low-speed path-following. The optimal design reduces the RWA (Rear-Ward Amplification) ratio in an obstacle avoidance lane change by 48.67 % from the baseline value, decreases the PFOT (Path-Following Off-Tracking) by 29.74 % from the baseline value.

Compared with the two design loop (TDL) design method reported in Ref. [12], the SDL approach searches solutions in a much larger design space and consequently it provides a more comprehensive set of optimal designs. This comprehensive set of optimal designs can be classified into three subsets, namely, RWA set for improving high-speed lateral stability, PFOT set for enhancing low-speed maneuverability, and Pareto set for optimal trade-off coordination between the high-speed stability and low-speed maneuverability. Simulation results illustrate that for the given design application, the SDL method offers better trade-off design solutions than the TDL approach. The proposed SDL method may be used for identifying desired design variables and predicting performance envelops in the early design stages of AHVs with ATS systems.

Chapter 6

A COMPOUND LATERAL POSITION DEVIATION PREVIEW CONTROLLER

6.1 INTRODUCTION

An optimal preview controller, called compound lateral position deviation preview (CLPDP) controller, is designed for active trailer steering (ATS) systems to improve high-speed stability of articulated heavy vehicles (AHVs). The main reason of many recently reported highway accidents is due to AHVs' unstable motion modes, including jack-knifing and rollover. To prevent these unstable motion modes, the optimal controller, namely the compound lateral position deviation preview controller (CLPDP) is proposed to control the steering of the front and rear axle tires of the trailing unit of a tractor/full-trailer combination. The corrective steering angle of the trailer front axle tires is determined using the preview information of the lateral position deviation of the trajectory of the axle center from that of the tractor front axle center. In turn, the steering angle of the trailer rear axle tires is calculated considering the lateral position deviation of the trajectory of the axle center from that of the trailer front axle. The linear quadratic regular technique is applied to the design of the proposed preview control scheme in the continuous time domain.

The rest of the chapter is organized as follows. Section 6.2 states the vehicle model and maneuver used in the design of the CLPDP controller for the ATS system of the tractor/full-trailer combination. The design of the controller is introduced in Section 6.3. Section 6.4 compares the simulation results based on the controller against those based on the baseline vehicle. Finally, conclusions are drawn in Section 6.5.

6.2 VEHICLE SYSTEM MODELS

6.2.1 Vehicle Model

The proposed CLPDP controller algorithm is developed and tested for a tractor/full-trailer combination. The 3-DOF linear vehicle model, i.e. Model-2, introduced in Subsection 3.2.2 will be used to evaluate the high-speed stability.

6.2.2 Maneuver Emulated

A single lane change maneuver is simulated for determining the high-speed RWA ratio. In the simulation, the vehicle is traveling at the speed of 88.0 km/h along a straight path and a sudden lane change is conducted. The lateral displacement of the vehicle in the lane change is 1.46 m. The steering input for this maneuver takes a single sinusoidal wave, as in equation (3.9), where the period T is 2.5 seconds and the value of amplitude A is selected in such a way that the vehicle is able to complete the single lane change.

6.3 CLPDP CONTROLLER DESIGN

6.3.1 Proposed Control Strategy

In the design of the compound lateral position deviation preview (CLPDP) controller, it is assumed that the path-following error between the front and rear axles of the tractor is negligible. The controller design is based on the basic concept: 1) the center of the trailer front axle tracks the path of the center of the tractor front axle; and 2) the center of the trailer rear axle tracks the path of the center of it front axle. The CLPDP controller with this basic design concept is intended to search for a better trade-off solution between the transient path- following and the lateral stability at high speeds.

As shown in Fig. 6.1, the controller should steer the trailer tires to minimize the lateral position deviation between the trailer front axle center trajectory, denoted as y_{f2} at the time instant t, and the tractor front axle center trajectory, represented as y_{f1} at the time instant $t - m\Delta t$. Here m takes an integer value, $\Delta\tau$ denotes the time increment, and $m\Delta t$ represents the time required for the vehicle to travel the distance between the front axle of the tractor and that of the trailer. This distance is calculated while the articulation angle ψ taking the value of zero. Moreover, the controller should determine the steering angles of the trailer tires to minimize the lateral position deviation between the trailer rear axle center trajectory, denoted as y_{r2} at the time instant t, and the trailer front axle center trajectory, represented as y_{f2} at the time instant $t - (n - m)\Delta\tau$. Note that if $\psi = 0$, $n\Delta\tau$ is the time required for the vehicle to travel the distance between the tractor front axle and the trailer rear axle and n is an integer.

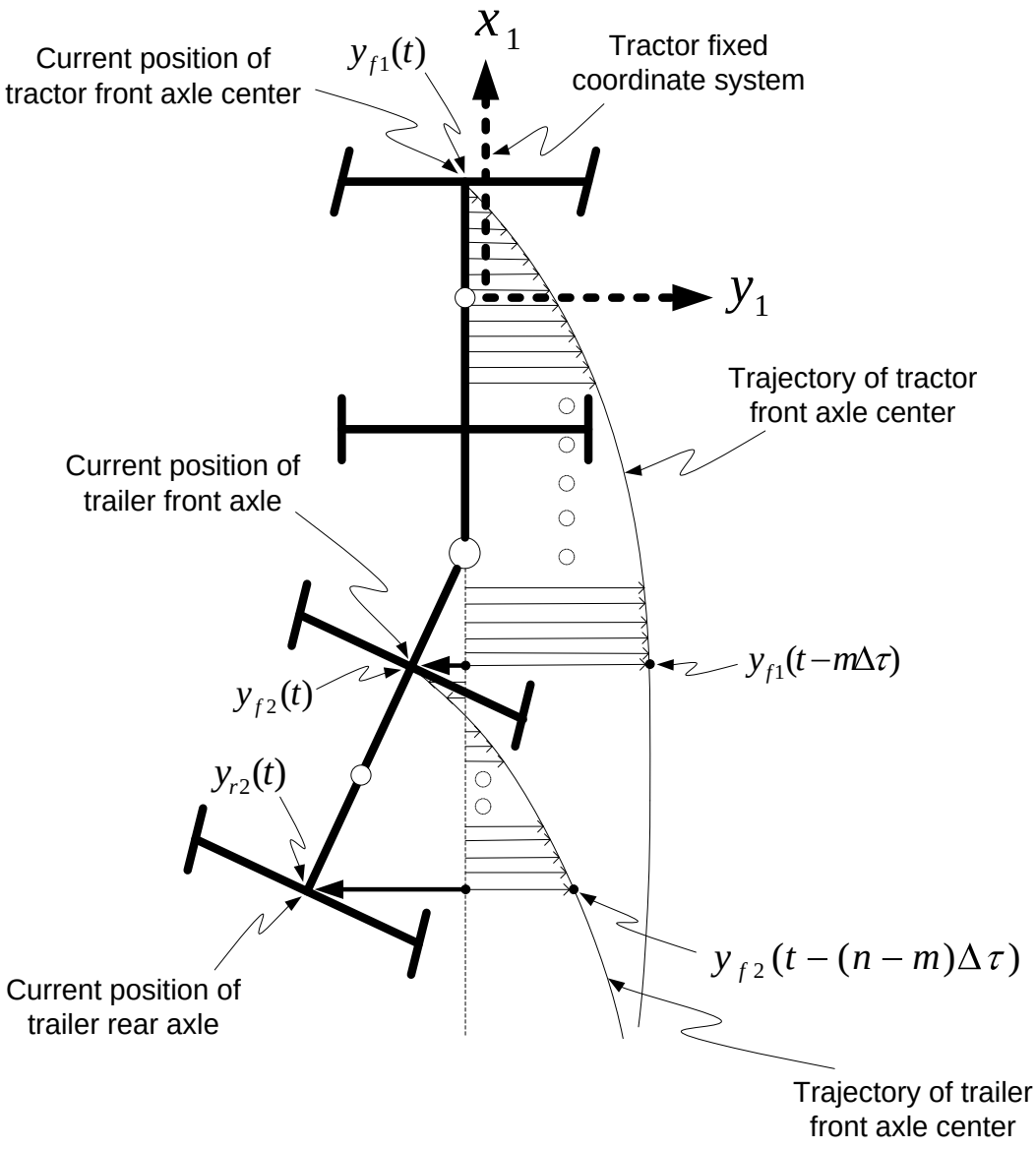

Fig. 6.1: Schematic diagram showing degrees of freedom and system parameters of vehicle model

6.3.2 Design Criteria

To implement the above strategy, the controller is designed based on the linear quadratic regulator (LQR) theory in the continuous time domain. The mathematical expression of cost function of the LQR controller is devised as follows

$$J = \int_0^\infty [q_1 \times \left(y_{f1}(t - m\Delta\tau) - y_{f2}(t)\right)^2 + q_2 \times \left(y_{f2}(t - (n-m)\Delta\tau) - y_{r2}(t)\right)^2 + q_3\left(y_{r2}(t)\right)^2 + q_4 \times \left(\delta_f(t)\right)^2 + q_5 \times \left(\delta_r(t)\right)^2]dt \tag{6.1}$$

The significance of each term of the above cost function can be described with the aid of Fig. 6.1. In the first term $y_{f1}(t - m\Delta\tau) - y_{f2}(t)$ represents the lateral position deviation of the trajectory of the tractor front axle center trajectory with respect to that of the trailer front axle center. The weighting factor q_1 imposes penalty upon the magnitude and direction of this deviation. This penalty implies that the ATS system should locate the current position of the trailer front axle center $y_{f2}(t)$ on the trajectory of tractor front axle center denoted as $y_{f1}(t - m\Delta\tau)$. Note that all the deviations are expressed in the body-fixed coordinate system of tractor.

Similarly the weighting factor q_2 punishes the magnitude and direction of the expression $y_{f2}(t - (n-m)\Delta\tau) - y_{r2}(t)$ as shown in the second term of cost function of equation (6.2). The physical meaning of this expression is that at any instant t, the current position of the trailer rear axle center $y_{r2}(t)$ should be on the trajectory of the trailer front axle center $y_{f2}(t - (n-m)\Delta\tau)$. Note that the time delay $(n-m)\Delta\tau$ represents the time

required for the trailer rear axle center to reach the current location of trailer front axle center.

In equation (6.2), q_3 is the weighting factor that imposes penalties upon the magnitude and duration of the lateral position deviation of the trailer rear axle center from the longitudinal axes of the tractor and trailer. The goal for introducing this term is to prevent the dangerous jack-knifing motion mode during lane change and tight curved path negation maneuvers. Note that the fourth and fifth terms on the right side of equation (6.2) represent the energy consumption of the active trailer steering system. Introducing these two terms will minimize the required energy consumption.

6.3.3 CLPDP Controller Design

Based on the design criteria in terms of the cost function expressed in equation (6.2), the 3-DOF vehicle model described in Subsection 3.2.2 cannot be incorporated directly in the design of the CLPDP controller. The vehicle model should be modified to include the required state variables: 1) lateral displacement of the tractor front axle center y_{f1}; 2) lateral displacement of the trailer front axle center y_{f2}; and 3) lateral displacement of the trailer rear axle center y_{r2}. Moreover, the modified vehicle model should consider the time delays $m\Delta\tau$ and $(n-m)\Delta\tau$ for the state variables y_{f1} andy_{f2}, respectively. The differential equations associated with the newly introduced state variables are constructed as follows,

$$\dot{y}_{f1} = V_1 + S_1\omega_1 \tag{6.2a}$$

$$\dot{y}_{f2} = V_2 + S_5\omega_2 \tag{6.2b}$$

$$\dot{y}_{r2} = V_2 - S_6\omega_2 \tag{6.2c}$$

The finite forward difference approximation of derivatives is considered to calculate these state variables with the time delays in the continuous time domain. Note that the similar approach was also used in the relevant linear time delayed system [11].

$$\dot{y}_{f1}(t - i\Delta\tau) = \frac{1}{\Delta\tau}\left[y_{f1}(t - (i-1)\Delta\tau) - y_{f1}(t - i\Delta\tau)\right], \quad \text{for } i = 1,2,\dots,m,\dots,n \tag{6.3a}$$

$$\dot{y}_{f2}(t - i\Delta\tau) = \frac{1}{\Delta\tau}\left[y_{f2}(t - (i-1)\Delta\tau) - y_{f2}(t - i\Delta\tau)\right], \quad \text{for } i = 1,2,\dots,(n-m) \tag{6.3b}$$

where both m and n take integer values and $m < n$. Note that the time delay for the lateral displacement of trailer rear axle center y_{r2} is not considered. Finally the combined linear dynamic model with two time delays is cast in state space form as follows

$$\dot{\mathbf{z}}(t) = \mathbf{A}_{pv}\mathbf{z}(t) + \mathbf{B}_{pv}\mathbf{u}(t) + \mathbf{C}_{pv}\delta(t) \tag{6.4}$$

where matrices $\mathbf{A}_{pv}$, $\mathbf{B}_{pv}$, and $\mathbf{C}_{pv}$ are provided in Appendix A. In the linear model of equation (6.5) the state variable sets $\mathbf{z}(t) \in \mathbf{R}^{(2n-\mathrm{m}+7)\times 1}$ are extended as

$$\begin{aligned}\mathbf{z}(t) = [\mathbf{x}(t)^{\mathrm{T}},\ & y_{f1}(t),\ y_{f1}(t-\Delta\tau),\ y_{f1}(t-2\Delta\tau),\cdots,\ y_{f1}(t-m\Delta\tau),\cdots,\\ & y_{f1}(t-n\Delta\tau),\ y_{f2}(t),\ y_{f2}(t-\Delta\tau),\ y_{f2}(t-2\Delta\tau),\cdots,\\ & y_{f2}(t-(n-m)\Delta\tau),\ y_{r2}(t)]^T\\ \equiv [\mathbf{z_1}(t),\ & \mathbf{z}_2(t),\ \mathbf{z}_3(t),\ \cdots,\ \mathbf{z}_{2n-m+7}(t)]^T\end{aligned} \tag{6.5}$$

By solving the algebraic Ricatti equation, the control matrix $\mathbf{K} \in \mathbf{R}^{2\times(2n-m+7)}$ can be determined and optimal trailer steering command vector $\mathbf{u}(t) \in \mathbf{R}^{2\times1}$ can be calculated as

$$\mathbf{u}(t) = -\mathbf{K}\,\mathbf{z}(t) \tag{6.6}$$

6.4 NUMERICAL SIMULATION

In this section, the simulation results of the AHV with the proposed CLPDP controller are examined and compared with those of the baseline vehicle. To make the results of both cases consistent and comparable, the testing maneuver introduced in Subsection 6.2.2 is simulated. Note that the baseline vehicle system parameters are offered in Appendix B and the trailer axles are non-steerable.

To examine the performance of the CLPDP controller, 50 path preview sample values are selected from the trajectory of the tractor front axle center, i.e. n takes the value of 50. With $\psi = 0$, the distance between the tractor front axle and the trailer rear axle is 10.06 m. If the vehicle travels at the forward speed, V_1, of 88.0 km/h, the time required for the trailer axle center to reach the current position of the tractor front axle center is $n\Delta\tau = 0.4115$ seconds. Thus, the time increment can be determined as $\Delta\tau = \frac{0.4115}{50} = 0.0082$ seconds. Similarly, with $\psi = 0$, the distance between the tractor front axle and the trailer rear axle is 7.01 m. The corresponding time delay can be easily determined as $m\Delta\tau = \frac{7.05}{24.4444} = 0.2868$ seconds. The required number of path preview sample values is

calculated through $m = \frac{0.2868}{\Delta\tau} = 34.9723 \cong 35$. Note that if m takes the nearest integer value, this may degrade vehicle performance. To minimize this negative impact, the total number of sample values n should take a large integer value. The weighting factor vector $[q_1 \quad q_2 \quad q_3 \quad q_4 \quad q_5]$ is assigned the value of [0.5672, 1.8437, 3.3753, 0.4867, 0.4702] using the weighting factor determination procedure reported in [13, 4].

The general goal of the CLPDP controller is to make the trailer to follow the tractor with adequate fidelity in a safe and stable manner. From stability point of view, the lower the RWA ratio, the better the stability. However, if the RWA ratio takes very small value, the trailer will not follow the path of the tractor. It is recommended that the RWA ratio take the value of 1.0 [1]. This RWA ratio may make the lateral accelerations for both the tractor and trailer comparable as well as comparable trajectories for both units.

Table 6.1: Selected simulation results for the baseline vehicle and the one with the CLPDP controller

	Baseline vehicle	**Vehicle with CLPDP controller**
RWA Ratio	1.2024	0.8980
Transient PFOT (m)	0.0631	0.0480
Steering sine-wave amplitude *A* (radian)	0.0044	0.0508

Table 6.1 offers the selected simulation results for the vehicle with the CLPDP controller and those for the baseline vehicle. The RWA ratio of the vehicle with the controller is 0.8980 and it is closer to the ideal value of 1.0 compared against the baseline

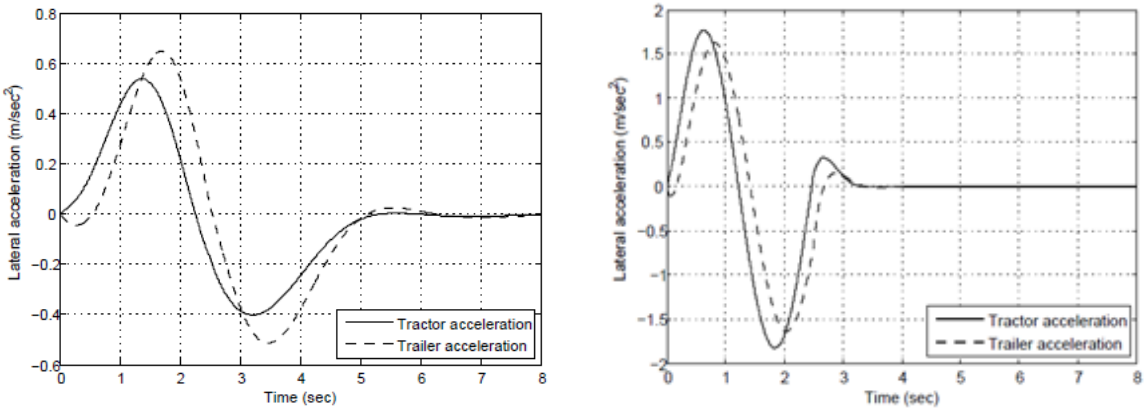

(a) (b)

Fig. 6.2: Lateral accelerations at tractor and trailer CG: (a) baseline case; and (b) control case

value of 1.2024. The transient PFOT of the controlled vehicle is 0.048 m, which is 23.8 % lower than the corresponding baseline value of 0.063 m. Fig. 6.2 shows the lateral accelerations at tractor CG and that of the trailer CG for both the baseline vehicle and the one with the controller. A close observation of the simulation results reveals that in the control case, the steady state response can be achieved in 3 s, whereas in the baseline case, 5 s is needed to obtain the corresponding steady state response.

Fig. 6.3 shows the trajectory of the tractor front axle center and that of the trailer rear axle center for both the baseline case and the control case. In the control case shown in Fig. 6.3(b), the vehicle is able to complete the lane change at the longitudinal distance of about 73m from the starting point, while the baseline vehicle needs a distance of around 155m to finish the lane change as shown in Fig. 6.3(a).

Fig. 6.4 illustrates the time history of the lateral displacement of the tractor front axle center and that of the trailer rear axle center for both the baseline case and control case.

In the control case, the tractor and trailer reach the lateral displacement of 1.46 m at 3.04 and 3.47 s, respectively, while in the baseline case, the tractor and trailer first achieve this

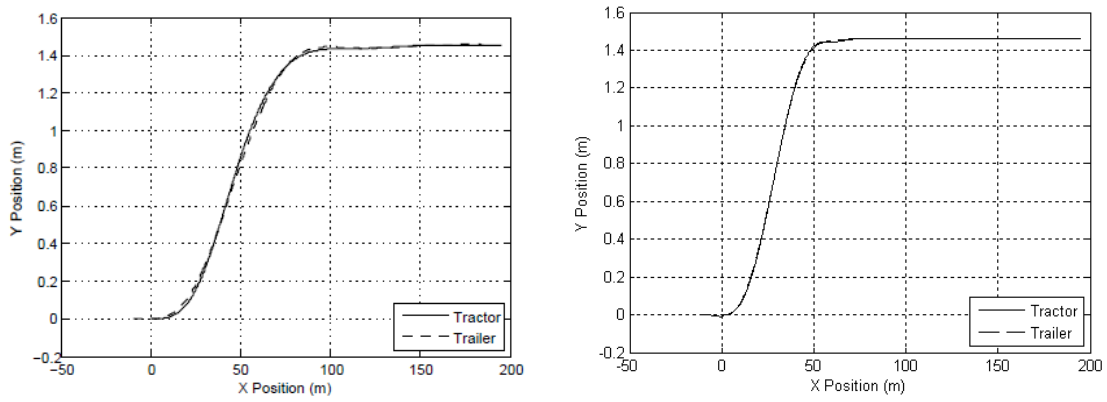

Fig. 6.3: Trajectories of tractor and trailer front axle center in global coordinate system: (a) baseline case; and (b) control case

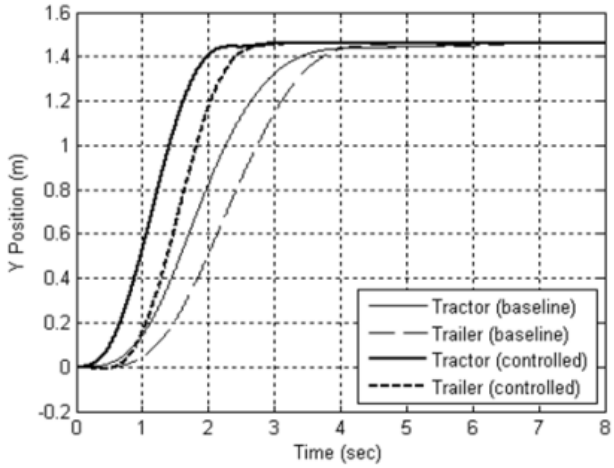

Fig. 6.4: Time history of lateral displacement of tractor front axle center and that of trailer rear axle center for baseline case and control case

lateral displacement at 6.30 s and 6.75 s, correspondingly. Thus, the vehicle with the controller can complete the lane change much faster than the baseline vehicle. Note that the vehicle with the CLPDP control achieves the above superior performance under the

condition of larger driver steering angle input than that used for the baseline vehicle as shown in Table 6.1.

6.5 CONCLUSIONS

This chapter presents a compound lateral position deviation preview (CLPDP) control scheme for active trailer steering (ATS) systems to improve high-speed stability of articulated heavy vehicles (AHVs). The proposed CLPDP controller has been designed using linear quadratic regulator (LQR) algorithm in the continuous time domain. To examine the performance of the controller, it has been applied to the design of a tractor/full-trailer combination with an ATS system. To perform numerical simulations, a 3 degree of freedom vehicle model is generated to represent the tractor/full-trailer system. The resulting design based on the controller is compared with the baseline vehicle. Numerical simulation results of a high-speed lane change maneuver show that the vehicle with the controller is superior to the baseline vehicle in the performance measures of high-speed lateral stability. In the case of control, the transient PFOT is reduced by 23.93% compared against the baseline value. The vehicle with the controller can complete the lane change much faster than the baseline vehicle, the former finishing this maneuver in about 3.47 seconds but the latter in 6.75 seconds. Moreover, the Rear-Ward Amplification ratio for the baseline case is 1.2024, while the corresponding value for the control case is 0.8980. Thus, the latter is closer to the ideal value of 1.0.

The above simulation results indicate that the CLPDP controller can improve the high-speed performance of the tractor/full-trailer combination. In the near future, the

effects of the controller on the low-speed performance of the vehicle system will be examined and evaluated.

Chapter 7

CONCLUSIONS

7.1 INTRODUCTION

As discussed and identified in Chapter 1, the ultimate objective of this thesis is to develop a novel method for the design method of articulated heavy vehicles (AHVs) with active trailer steering (ATS) systems. The numerical simulation results reveal that the goal has been successfully achieved. The feasibility and efficacy of the method has been demonstrated by optimizing the high-speed stability and low-speed maneuverability of a tractor/full-trailer combination. This design synthesis method and the numerous conclusions drawn from the above numerical experiments are believed to be important contributions to the design optimization of articulated heavy vehicles with active steering systems.

In this chapter, the achievements of the research are addressed and the related areas for future research are proposed.

7.2 PROPOSED SYNTHESIS METHOD

In the thesis, a single design loop (SDL) method has been compared with a two design loop (TDL) method through the design synthesis of a tractor/full-trailer with an ATS system. Compared with TDL method, the SDL approach searches solutions in a much

larger design space and consequently it provides a more comprehensive set of optimal designs. This comprehensive set of optimal designs can be classified into three subsets

- RWA (Rear-Ward Amplification) set for improving high-speed lateral stability
- PFOT (Path-Following Off-Tracking) set for enhancing low-speed maneuverability
- Pareto set for optimal trade-off condition between the high-speed stability and low-speed maneuverability

The simulation results illustrate that for the given design application, the SDL method offers better trade-off design solutions than the TDL approach.

The SDL method can be used to automate the process of determining optimal values of design for improving compatibility of the fundamental conflicting design criteria of AHVs, i.e. low-speed maneuverability and high-speed stability. The SDL method has the following distinguished features:

1. The optimal active design variables of ATS systems and optimal passive vehicle system design variables are searched in a single design loop,
2. In the design process, to evaluate the vehicle performance measures a driver model is developed and it ‘drive’ the vehicle model based on the well-defined testing specifications, and

3. The ATS controller designed from this method has two operational methods; one for improving the lateral stability at high speeds, and the other for enhancing path-following at low speeds.

The proposed SDL method may be used for identifying desired design variables and predicting performance envelops in the early design stages of AHVs with ATS systems.

7.3 COMPOUND LATERAL POSITION DEVIATION PREVIEW CONTROLLER

This thesis also proposed, developed and tested a compound lateral position deviation preview (CLPDP) controller for ATS systems of AHVs to improve high-speed stability. The proposed controller has the following features:

- It is designed using linear quadratic regulator (LQR) algorithm in the continuous time domain,
- Time delay is taken into account to control the relevant trailer axle tires, and
- The controller utilizes a compound set of preview information of the lateral position deviation.

The numerical simulation results of a high-speed lane change maneuver show that the vehicle with the controller is superior to the baseline vehicle in the performance measures of high-speed lateral stability.

7.4 DIRECTIONS FOR FUTURE RESEARCH

To improve the proposed design synthesis method for AHVs with ATS system, the following directions for future research are recommended.

1. **Implementation in Parallel Computations Environment.** The method is suitable for applications using massively-parallel computers and the computation time could be reduced approximately by a factor of the population size of the GA [8].

2. **Application to the Design Optimization of AHVs with Integrated Control Systems.** The anti-lock braking system, all tire steering system, and active suspension system are based on three different directions of road vehicle dynamics, i.e. longitudinal, lateral, and vertical respectively. The proposed method is readily applicable to the design of AHVs with an integrated control system where the three control systems can co-operate each other. Moreover, the mechanical system and control system of AHV, with the method, can be optimized simultaneously.

The limitation of the application of the proposed method is that the associated computational burden is heavy. However, parallel processing, for which the method is ideally suited, could be used for decreasing the total computer time required for the optimization.

Although the method was originally intended for the design optimization of articulated heavy vehicles (AHVs) with active trailer steering (ATS) system, this general

design method is also applicable to the design of other complex dynamic systems, e.g. robots, and the other mechatronic systems, with minor modifications.

Bibliography

[1] Fancher, P. and Winkler, D. 2007. Directional performance issues in evaluation and design of articulated heavy vehicles, *Vehicle System Dynamics*, 45(7-8), 607-647,.

[2] Vlk, F. 1985. Handling Performance of Truck-Trailer Vehicles: A State-of-the-Art Survey, *Int. J. Of Vehicle Design* 6(3), 323-361.

[3] Chen, B. and Peng, H. 1999. Rollover Warning For Articulated Vehicles Based on A Time-To-Rollover Metric", *ASME International Mechanical Engineering Conference and Exhibition*, November.

[4] El-Gindy, M., Mrad, N. and Tong, X. 2001. Sensitivity of rearward amplification control of a tractor/full trailer to tyre cornering stiffness variable, *Proc. IMechE, Part D*: *J. Automobile Engineering*, 215, 579-588.

[5] National Highway Traffic Safety Administration: Traffic Safety Facts 1993 - 1998: A Compilation of Motor Vehicle Crash Data from the Fatality Analysis Reporting System and the General Estimates System, 1994 - 1999.

[6] Gerum, E., Laszlo, P., Semsey, A., and Barta, G. 1998. Method for drive stability enhancement of multi-unit vehicles. U.S. Patent 5 747 683, May 5.

[7] Anderson, R., Elkins, J. And Brickle, B. 2001. Rail Vehicle Dynamics for the 21th Century", *Proceedings of ICTAM*'2000, Chicago, USA.

[8] He, Y. 2003. Design of Rail Vehicles with Passive and Active Suspensions Using Multidisciplinary Optimization, Multibody Dynamics, and Genetic Algorithms", PhD thesis, University of Waterloo, Waterloo, Ontario, Canada.

[9] He, Y. 2005. Khajepour, A., McPhee, John, and Wang, X., "Dynamic Modeling and Stability Analysis of Articulated Frame Steer Vehicles. *Int. J. Of Heavy Vehicle Systems*, 12(1), 28-59.

[10] Islam, M.M., and He, Y. 2008. Stability Optimization of Articulated Frame Steer Vehicles", 2nd CIRP Conference on Assembly Technologies and Systems, Toronto, Canada.

[11] Islam, M. and He, Y. 2009. Design synthesis of heavy articulated vehicles with rearward amplification control, In Proceedings of the 22nd Canadian Congress of Applied Mechanics, Dalhousie University, Halifax, Canada, pp. 131-132.

[12] He, Y., Islam, M.M. and Webster, T.D. 2010. An integrated design method for Articulated Heavy Vehicles with Active Trailer Steering Systems", accepted by SAE 2010 World Congress, SP-2261, SAE paper No. 2010-1-0092.

[13] Islam, M.M., He, Y., and Webster, T.D. 2010. Automated design synthesis of articulated heavy vehicles with active trailer steering systems", accepted by ASME IDETC/CIE 2010, Paper No: DETC2010-28160.

[14] Wu, D.H. 2001. A Theoretical Study of the Yaw/Roll Motions of A Multiple Steering Articulated Vehicle, *Proceedings Institutions of Mech. Engg.*, Vol. 215, Part D.

[15] Winkler, C.B., Blower, D., Ervin, R.D. and Chalasani, R.M. 2000. Rollover of Heavy Commercial Vehicles", SAE, Warrendale, PA, USA.

[16] Miege, A.J.P. 2003. Active Roll Control of an Experimental Articulated Vehicle. Cambridge University Engineering Department, PhD Dissertation.

[17] Anon. 2002. Road Accidents in Great-Britain. Department of Transport, HMSO, UK.

[18] Rakheja, S., Sankar, S. and Ranganthan, R. 1987. Roll plane analysis of articulated tank vehicles during steady turning. *Vehicle System Dynamics*, 17(2), pp. 81–104.

[19] Broge, J.L. 2000. Heavy duty truck safety systems. *Automotive Engineering International*, pp. 101–105.

[20] Anon. 2001. Traffic Safety Facts 2000: A compilation of motor vehicle crash data from the Fatality Analysis Reporting System and the General Estimates System. Technical Report DOT HS 809 337, National Highway Traffic Safety Administration, National Center for Statistics and Analysis, Washington DC, USA.

[21] Erkert, T.W., Sessions, J., Layton,R.D. 1989. A Method for Determining off-tracking of multiple unit vehicle combinations", *Int. J. Of Forest Engg.*, 1989.

[22] He, Y., Khajepour, A., McPhee, J. and Wang, X. 2005. Dynamic modelling and stability analysis of articulated frame steer vehicles, *Int. J. Heavy Vehicle Systems*, 12(1), 28-59.

[23] He, Y. and McPhee, J. 2005. A design method for mechatronic vehicles: application of multidisciplinary optimization, multibody dynamics and genetic algorithms", *Vehicle System Dynamics*, 43(10), 697-733.

[24] Christensen, T.C., and Blythe, W. 2000. Offtracking: History, Analysis, and Simulation, *SAE 2000 World Congress*, 2000-01-0465, Detroit, MI, USA, March.

[25] Palkovics, L. and Fries, A. 2001. Intelligent electronic systems in commercial vehicles for enhanced traffic safety, *Vehicle System Dynamics*, 35(4-5), 227-289.

[26] Prem, H., Ramsay, E., Pont, J., McLean, J. and Woodrooffe, J. 2001. Comparison of modelling systems for performance-based assessments of heavy vehicles (Performance based standards – NRTC/Austroads project A3 and A4), The National Road Transport Commission (NRTC), Working Paper, October.

[27] Winkler, C.B., Fancher, P.S., Bareket, Z., Bogard, S.E., Johnson, G., Karamihas, S.M. and Mink, C.E. 1992. Heavy vehicle size and weight: test procedures for minimum safety performance standards. Final technical report", *Transportation Research Institute, Michigan University: Ann Arbor*, 118 p. UMTRI-92-13/DTNH-22-87-D-17174.

[28] Odhams, A., Roebuck, R., Cebon, D. and Winker, C. 2008. Dynamic safety of active trailer steering systems, *Proc. IMechE*, *Part K*: *J. Multi-body Dynamics*, 222, 367-380.

[29] Rangavajhula, K. and Tsao, H-S. J. 2007. Active steering control of an articulated system with a tractor and three full trailers for tractor-track following, *Int. J. Heavy Vehicle Systems*, 14(3), 271-293.

[30] Rangavajhula, K. and Tsao, H-S. J. 2008. Command steering of trailers and command-steering-based optimal control of an articulated system for tractor-track following, *Intn. Mech. Engrs.*, Vol.222, 2008. *Proc. IMechE, Part D*: *J. Automobile Engineering*, 222, 935-954.

[31] Aurell, J. and Edlund, S. 1989. The Influence of Steered Axles on the Dynamic Stability of Heavy Vehicles, *SAE paper* No. 892498.

[32] Jujnovich, B. and Cebon, D. 2002. Comparative performance of semi-trailer steering systems. In proceedings of the 7th International Symposium on Heavy Vehicle Weights and Dimensions, Delft, pp. 195-214.

[33] Wu, D-H. and Lin, J. H. 2003. Analysis of dynamic lateral response for a multi-axle-steering tractor and tractor and trailer", *Int. J. of Heavy Vehicle Systems*, 10(4), 281-294.

[34] Ellis, J. R. 1969. Vehicle Dynamics, Business Books Limited, London.

[35] Society of Automotive Engineers, A test for evaluating the rearward amplification of multi-articulated vehicles, SAE Recommended Practice J2179, SAE, Warrendale, USA, 1994.

[36] *Rules for the Assessment of Potential Performance-Based Standards.* Discussion Paper. National Transport Commission (NTC), Australia, June 2005.

[37] Bryson, A. and Ho, Y. 1975. Applied optimal control, optimization, estimation and control, Wiley, New York.

[38] Karnopp, D. 1990. Design principles for vibration controls systems using semi-active dampers, *Journal of Dynamics Systems Measurement Control*, 112, 448-455.

[39] Goldberg, D. 1989. Genetic algorithms in search, optimization, and machine learning, Addison-Wesley, Reading, MA.

[40] Thompson, A.G. 1976. An Active Suspension with Optimal Linear State Feedback, *Vehicle System Dynamics*, 5, 187-203.

[41] Palkovics, L., Semsey, A. and Gerum, E. 1998. Roll-Over Prevention System for Commercial Vehicles – Additional Sensorless Function of the Electronic Brake System. AVEC'98, Paper No. 9837409.

[42] "Truck and Bus Crash Factbook. 1995. University of Michigan Transportation Research Institute, Center for National Truck Statistics, UMTRI-97-30.

[43] Sankar, S., Rakhija, S. and Piche, A. 1991.Directional dynamics of a tractor – semi-trailer with self and force steering axles, *SAE Transactions*, SAE 912686.

[44] Lewis, A.S. and El-Gindy, M. 2003. Sliding mode control for rollover prevention of heavy vehicles based on lateral acceleration", Heavy Vehicle Systems, A Special Issue of the Int. J. of Vehicle Design, Vol. 10, Nos. 1/2, pp. 9–34.

[45] Harwood, D.W., Potts, I.B., Torbic, D.J., and Glauz, W.D. 2003. Highway/Heavy Vehicle Interaction", *Commercial Truck and Bus Safety Synthesis Program* CTBSSP-SYN-3, ISBN-0-309-08756-2. Washington, DC: Transportation Research Board.

[46] Fenwick SV, Harris JapC. 1999. The application of Pareto frontier methods in the multidisciplinary wing design of a generic modern military delta aircraft. In proceedings of NATO RTO AVT symposium, Ottawa, October.

[47] Abbass, H A, Sarker, R, and Newton C. 2001. PDE: A Paretofrontier differential evolution approach for multi-objective optimization problems", *Proc. of IEEE Congress on Evolutionary Computation.* pp 971-978.

[48] J. Cao, J. Lin. 2008. A Study on Formulation of Objective Functions for Determining Material Models", *Int. J. Mech. Sci.*, 50: 193-204, 2008.

[49] Rangavajhula, K. and Tsao, H.-S. J. Effect of multi-axle steering on off-tracking and dynamic lateral response of articulated tractor–trailer Combinations. Int. J. Heavy Veh. Systems, 14(4), 376–401.

[50] Tsao, H.-S. J., Dessouky, Y., Rangavajhula, K., Zeta, J. B., and Zhou, L. 2006. Automatic steering for conventional truck trailers: development and assessment of operating concepts for improving safety, productivity and pavement durability – final report, PATH Research Report UCB-ITS-PRR-2006- 8, Institute of Transportation Studies, University of California, Berkeley.

[51] *Road Vehicles–Heavy Commercial Vehicle Combinations and Articulated Buses-Lateral Stability Test Methods* (2nd edn) (International Organization for Standardization: Geneva, Switzerland), 12 p. ISO 14790:2000(E).

[52] A test for evaluating the rearward amplification of multi-articulated vehicles. Standard J2179, Society of Automotive Engineers, September 1993.

[53] MacAdam, C.C. 1988. Development of driver/vehicle steering interaction models for dynamic analysis," Tech. Rep. U.S. Army Tank–Automotive Command, Univ. Michigan Transportation Res. Inst., Report UMTRI-88-53.

[54] Prem, H., Ramsay, E.D., De Pont, J., McLean, J.R. and Woodrooffe, J.H. 2001b. *Comparison of Modelling Systems for Performance-Based Assessments of Heavy Vehicles,* Working Paper prepared for the National Road Transport Commission

by RTDynamics, TERNZ Ltd, J.R. McLean and Woodrooffe & Associates Inc, Melbourne, Vic. October.

[55] DiCristoforo, Rob, Blanksby, Chris, and Germanchev, 2006. Anthony. *Performance-Based Certification of an Innovative Truck-Trailer Configuration for the Safer and More Efficient Distribution of Liquid Fuel in Australia*. ARRB Group Ltd., written for the Transportation Research Board Annual Meeting, Washington, D.C.

[56] Cohen, H. 2009. Wisconsin Truck Size and Weight Study, Wisconsin Department of Transportation.

[57] Tanaka K, Kosaki T. 1997 Design of a stable fuzzy controller for an articulated vehicle", *IEEE Trans Syst Man Cybern B Cybern*,27(3):552-8.

[58] Winkler, C. B., P. Fancher, P. S., Carsten, O., Mathew, A., Dill, P. 1986. Improving The Dynamic Performance Of Multitrailer Vehicles: A Study Of Innovative Dollies", Transportation Research Institute (UMTRI), University of Michigan, Ann Arbor.

[59] Fancher, P., Winkler, C., Ervin, R. and Zhang, H. 1997. Using Braking to Control the Lateral Motions of Full Trailers", The Dynamics of Vehicle on Roads and on Tracks. *Proceedings of the 15th IAVSD Symposium*, Budapest, Hungary, August 25-29, pp. 462-478.

[60] Antoniou, A ., and Lu, W-S. 2007. Practical optimization: algorithms and engineering applications", Springer, New York.

[61] Fakhreddine, O.K., and Clarence, D.S. 2004. Soft Computing and Intelligent Systems Design", Pearson, Harlow (UK).

[62] Holland, J. 1975. Adaptation in Natural and Artificial Systems", *University of Michigan Press*, Ann Arbor.

[63] Kalman, R.E. 1960. Contribution to the Theory of Optimal Control", *Bol. Soc. Matem. Maxico*, 102-119.

[64] Kalman, R.E. 1964. When is a Linear Control System Optimal?", *ASME transactions Series D (Journal of Basic Engineering)*, 51-60.

[65] Dutta, A., Bhattacharya, S., Keel, L.H. 2009. Linear Control Theory: Structure, Robustness and Optimization", *CRC press*, Florida.

[66] Janson, B.N., Awad, W., Robles, J., Kononov, J. and Pinkerton, B. 1998. Truck accidents at freeway ramps: data analysis and high-risk site identification", Journal of Transportation and Statistics, 75-92, January.

[67] Sharp, R. S. 2005. Driver steering control and a new perspective on car handling qualities", Proc. IMechE, Part C: J. Mechanical Engineerig Science, vol. 219, pp. 1041-1051.

[68] Sun, J. Q., and Song, B. 2009. Control Studies of Time-Delayed Dynamical Systems with the Method of Continuous Time Approximation", *Communications in Nonlinear Science and Numerical Simulation*, vol. 14, pp. 3933-3944.

[69] Cheng, C., and Cebon, D. 2008. Improving roll stability of articulated heavy vehicles using active semi-trailer steering", *Vehicle System Dynamics*, vol. 46, pages 373-388.

APPENDEX

APPENDIX A: VEHICLE MODEL SYSTEM MATRICES

$$\mathbf{A}_{pv} = \begin{bmatrix} \mathbf{A} & \mathbf{0} & \mathbf{0} & \mathbf{0} \\ \mathbf{A_{f1}} & \mathbf{0} & \mathbf{0} & \mathbf{0} \\ \mathbf{0} & \mathbf{A_{pf}} & \mathbf{0} & \mathbf{0} \\ \mathbf{A_{f2}} & \mathbf{0} & \mathbf{0} & \mathbf{0} \\ \mathbf{0} & \mathbf{0} & \mathbf{A_{pr}} & \mathbf{0} \\ \mathbf{A_{r2}} & \mathbf{0} & \mathbf{0} & \mathbf{0} \end{bmatrix}_{(2n+7-m)\times(2n+7-m)}$$

$$\mathbf{B}_{pv} = \begin{bmatrix} \mathbf{B} \\ \mathbf{0} \end{bmatrix}_{(2n+7-m)\times 2}$$

$$\mathbf{C}_{pv} = \begin{bmatrix} \mathbf{C_2} \\ \mathbf{0} \end{bmatrix}_{(2n+7-m)\times 1}$$

where matrices $\mathbf{A_{f1}}$, $\mathbf{A_{f2}}$, $\mathbf{A_{r2}}$, $\mathbf{A_{pf}}$, $\mathbf{A_{pr}}$, **A, B,** $\mathbf{C_2}$, **(**and also $\mathbf{C_1}$ for Model-1) are defined as follows

$$\mathbf{A_{f1}} = [1 \quad S_1 \quad 0 \quad 0]$$

$$\mathbf{A_{f2}} = [1 \quad -(d+e-S_5) \quad S_4 \quad U_1]$$

$$\mathbf{A_{r2}} = [1 \quad -(d+e+S_6) \quad e+S_6 \quad U_1]$$

$$\mathbf{A_{pf}} = \begin{bmatrix} \frac{1}{\Delta\tau} & -\frac{1}{\Delta\tau} & 0 & \dots & 0 \\ & & \ddots & & \\ & & & \ddots & \\ 0 & \dots & 0 & \frac{1}{\Delta\tau} & -\frac{1}{\Delta\tau} \end{bmatrix}_{n\times n}$$

$$\mathbf{A_{pr}} = \begin{bmatrix} \frac{1}{\Delta\tau} & -\frac{1}{\Delta\tau} & 0 & \dots & 0 \\ & & \ddots & & \\ & & & \ddots & \\ 0 & \dots & 0 & \frac{1}{\Delta\tau} & -\frac{1}{\Delta\tau} \end{bmatrix}_{(n-m)\times(n-m)}$$

$$\mathbf{A} = \mathbf{M^{-1}N}$$

$$\mathbf{B} = \mathbf{M^{-1}P}$$

$$\mathbf{C_1} = \mathbf{M^{-1}L_1}$$

$$\mathbf{C_2} = \mathbf{M^{-1}L_2}$$

The matrices **M**, **N**, **P**, $\mathbf{L}_1$, and $\mathbf{L}_2$ are given below

$$\mathbf{M} = \begin{bmatrix} m_1 + m_2 & -m_2 d - m_2 e & m_2 d + m_2 e & 0 \\ -m_2 d & m_2 e(d+e) + I_1 & -m_2 e(d+e) & 0 \\ -m_2 e & m_2 e(d+e) + I_2 & -m_2 e(d+e) - I_2 & 0 \\ 0 & 0 & 0 & 1 \end{bmatrix}$$

$$\mathbf{N} = \begin{bmatrix} n_{11} & n_{12} & n_{13} & n_{14} \\ n_{21} & n_{22} & n_{23} & n_{24} \\ n_{31} & n_{32} & n_{33} & n_{34} \\ 0 & 0 & 1 & 0 \end{bmatrix}$$

$$\mathbf{P} = \begin{bmatrix} -C_1 \\ -C_1 S_1 \\ 0 \\ 0 \end{bmatrix}$$

$$\mathbf{L_1} = \begin{bmatrix} -C_3 \\ C_3 d \\ C_3(e - S_5) \\ 0 \end{bmatrix}$$

$$\mathbf{L_2} = \begin{bmatrix} -C_3 & -C_4 \\ C_3 d & C_4 d \\ C_3(e - S_5) & C_4(e + S_6) \\ 0 & 0 \end{bmatrix}$$

In matrices **M**, **N**, **P**, $\mathbf{L_1}$, and $\mathbf{L_2}$, the relevant elements are given as:

$d = S_2 + S_3$, $e = S_4 + S_5$,

$n_{11} = \frac{C_1+C_2+C_3+C_4}{U_1}$,

$n_{12} = \frac{C_1S_1-C_2S_2-C_3(d+e-S_5)-C_4(d+e+S_6)}{U_1} - (m_1 + m_2)U_1$,

$n_{13} = \frac{C_3(d+e-S_5)+C_4(d+e+S_6)}{U_1}$,

$n_{14} = C_3 + C_4$,

$n_{21} = \frac{C_1S_1-C_2S_2-C_3d-C_4d}{U_1}$,

$n_{22} = \frac{C_1S_1^2+C_2S_2^2+C_3d(d+e-S_5)+C_4d(d+e+S_6)}{U_1} + m_2dU_1$,

$n_{23} = \frac{-C_3d(d+e-S_5)+C_4d(d+e+S_6)}{U_1}$,

$n_{24} = -d(C_3 + C_4)$,

$n_{31} = -\frac{C_3(e-S_5)+C_4(e+S_6)}{U_1}$,

$n_{32} = \frac{C_3(e-S_5)(d+e-S_5)+C_4(e+S_6)(d+e+S_6)}{U_1} + m_2eU_1$,

$n_{33} = -\frac{C_3(e-S_5)(d+e-S_5)+C_4(e+S_6)(d+e+S_6)}{U_1}$,

$$n_{34} = -C_3(e - S_5) - C_4(e + S_6)$$

APPENDIX B: VEHICLE MODEL SYSTEM PARAMETERS

Table B1: Nominal values for the baseline tractor/full-trailer system [30]

Notation	Value	Unit	Notation	Value	Unit
m_1	6825	kg	m_2	5460	kg
I_1	21693	kg·m/s^2	I_2	12540	kg·m/s^2
S_1	2.56	m	S_2	1.10	m
S_3	0.91	m	S_4	2.44	m
S_5	1.68	m	S_6	1.37	m
C_1	-131364	N/rad	C_2	-262730	N/rad
C_3	-152032	N/rad	C_4	-152032	N/rad

Note: the absolute values for C_1, C_2, C_3 and C_4 are twice the amount of those given in Ref. [30].